

# Parsimonious sediment transport equations based on Bagnold's stream power approach

Roderick W. Lammers<sup>1\*</sup>  and Brian P. Bledsoe<sup>2</sup>

<sup>1</sup> Department of Civil and Environmental Engineering, Colorado State University, Fort Collins, CO USA

<sup>2</sup> College of Engineering, University of Georgia, Athens, GA USA

Received 1 March 2017; Revised 7 August 2017; Accepted 21 August 2017

\*Correspondence to: Roderick W. Lammers, Department of Civil and Environmental Engineering, Colorado State University, Fort Collins, CO, USA. E-mail: rodlammers@gmail.com



Earth Surface Processes and Landforms

**ABSTRACT:** It is increasingly recognized that effective river management requires a catchment scale approach. Sediment transport processes are relevant to a number of river functions but quantifying sediment fluxes at network scales is hampered by the difficulty of measuring the variables required for most sediment transport equations (e.g. shear stress, velocity, and flow depth). We develop new bedload and total load sediment transport equations based on specific stream power. These equations use data that are relatively easy to collect or estimate throughout stream networks using remote sensing and other available data: slope, discharge, channel width, and grain size. The new equations are parsimonious yet have similar accuracy to other, more established, alternatives. We further confirm previous findings that the dimensionless critical specific stream power for incipient particle motion is generally consistent across datasets, and that the uncertainty in this parameter has only a minor impact on calculated sediment transport rates. Finally, we test the new bedload transport equation by applying it in a simple channel incision model. Our model results are in close agreement to flume observations and can predict incision rates more accurately than a more complicated morphodynamic model. These new sediment transport equations are well suited for use at stream network scales, allowing quantification of this important process for river management applications. Copyright © 2017 John Wiley & Sons, Ltd.

**KEYWORDS:** stream power; sediment transport; catchment scale; Bagnold

## Introduction

Geomorphologists and engineers spent the last century developing empirical and process-based formulae for modeling sediment transport in rivers. Unfortunately, these formulae are data intensive and difficult to apply at larger spatial scales and in data poor environments. Managers and researchers recognize the importance of understanding sediment dynamics at the catchment scale (Owens, 2005), but existing sediment transport formulae are not well suited for this type of application. This catchment scale approach is necessary for numerous management issues, including assessing channel erosion and deposition potential (Lea and Legleiter, 2016), estimating flood risk (Stover and Montgomery, 2001), protecting benthic habitat (Newson and Newson, 2000; Rice et al., 2001), and restoring natural sediment regimes (Wohl et al., 2015). In this paper, we present new sediment transport equations that use readily collected and widely available data for application to these challenging problems.

Many sediment transport equations rely on shear stress (requiring flow depth) (Meyer-Peter and Müller, 1948; Parker, 1990) or velocity (Brownlie, 1982) or both (Engelund and Hansen, 1967). Although these variables are physically linked to sediment transport processes, their temporal and spatial variability makes them difficult to measure or model. This difficulty in quantifying flow depth and velocity makes it challenging to apply equations based on these variables at the catchment scale.

An alternative variable is specific stream power:

$$\omega = \frac{\Omega}{w} = \frac{\rho g Q S}{w} \quad (1)$$

where  $\Omega$  is unit-length stream power ( $\text{W m}^{-1}$ ),  $w$  is channel width (m),  $Q$  is discharge ( $\text{m}^3 \text{s}^{-1}$ ), and  $\omega$  is specific stream power ( $\text{W m}^{-2}$  or equivalently  $\text{N m}^{-1} \text{s}^{-1}$ ). Specific stream power is relatively straightforward to estimate throughout river basins using remote sensing data to quantify channel slope and width and stream gages, hydrologic models, or regional empirical relationships to quantify discharge (Reinfelds et al., 2003; Phillips and Desloges, 2014). Stream power mapping has been successfully used to identify erosional and depositional areas (Bazzi and Lerner, 2015; Parker et al., 2015); however, quantitative estimates of sediment transport capacity may be needed to answer river management questions. The sediment transport equations developed in this study address this gap.

Others have recognized the benefits of a stream power approach to sediment transport modeling and several existing sediment transport equations use specific stream power. The most widely used of these is the Bagnold (1980) empirical bedload equation; however, this equation also relies on flow depth, directly and indirectly through calculation of the critical specific stream power for incipient motion. This renders the equation impractical to apply throughout a stream network. In

this paper, we adapted the Bagnold bedload equation – eliminating its dependence on flow depth – and developed a total load equation using the same set of variables.

The proliferation of sediment transport equations has been criticized as excessive – ‘there appears to be more bed load formulae than there are reliable data sets by which to test them’ (Gomez and Church, 1989) – and the development of yet another equation may be unwelcome. Sediment transport formulae, however, should be considered part of a toolbox, where each tool has its own purpose. While we add more equations to the toolbox, they have a specific role that is currently unfulfilled – to model sediment transport where only limited data are available.

This paper has three objectives. First, we test several methods to estimate critical specific stream power for incipient motion. We show that a simple approach using only sediment grain size (Parker et al., 2011) is as accurate as more data intensive methods. Second, we develop new bedload and total load formulae based on Bagnold’s stream power approach but with no flow depth term. We examine the sensitivity of these new equations and show the most difficult to quantify variables (grain size and dimensionless critical specific stream power) have the smallest influence on calculated transport rates. Third, we use our bedload equation in a simple channel incision model and show it is as accurate as a physically detailed morphodynamic model. These new transport equations are accurate and rely on variables that are easy to quantify at network scales, making them suitable for a wide array of catchment management applications.

## Background

### Limitations of shear stress-based transport equations

Sediment transport equations generally follow a consistent pattern. Some measure of the excess available force or energy of the flowing water (i.e. total force less some critical force for incipient motion) is directly related to sediment transport rates. Many equations use excess shear stress (Meyer-Peter and Müller, 1948; Parker et al., 1982; Wilcock and Crowe, 2003) where critical shear stress is often expressed in dimensionless form, also known as the Shields parameter ( $\theta_c$ ; Shields, 1936):

$$\theta_c = \frac{\tau_c}{(\rho_s - \rho)gD_s} = \frac{hs}{(s-1)D_s} \quad (2)$$

where  $\tau_c$  is critical shear stress (Pa),  $\rho_s$  and  $\rho$  are sediment and fluid density ( $\text{kg m}^{-3}$ ),  $g$  is gravitational acceleration ( $\text{m s}^{-2}$ ),  $h$  is flow depth (m),  $S$  is water surface slope ( $\text{m m}^{-1}$ ),  $D_s$  is a representative grain size (m, usually assumed to be the median grain size,  $D_{50}$ ), and  $s$  is the sediment specific gravity (assumed to be 2.65). Shear stress and the Shields parameter rely on flow depth, a limitation for quantifying incipient motion in data poor areas or throughout stream networks. Depth may be calculated using discharge and a flow resistance equation, but this approach relies on assumptions of channel geometry which are not always applicable (Recking, 2013).

In addition to relying on flow depth, another downside of using the Shields parameter is its tendency to increase with channel slope (Lamb et al., 2008; Recking, 2009; Parker et al., 2011; Camenen, 2012; Ferguson, 2012) which could cause over-prediction of sediment transport rates in steep streams. Stream power based sediment transport equations may be more accurate in these cases because dimensionless critical specific stream power may be uncorrelated with slope (Ferguson, 2005; Parker et al., 2011).

Despite its popularity, shear stress may not be the most appropriate basis for sediment transport equations. In a comprehensive analysis, specific stream power was shown to be more correlated with bedload transport rates than either shear stress or velocity (Parker, 2010; Parker et al., 2011). Excess specific stream power to the 3/2 power – without any other variables – predicted bedload transport rates with an  $R^2$  value of 0.656 (Martin and Church, 2000), further demonstrating the strength of this variable for sediment transport modeling. In a comparison study using data from a gravel-bed Austrian river, stream power equations were shown to perform markedly better than shear stress formulae (Habersack and Laronne, 2002). Shear stress may be more physically representative of sediment transport mechanisms than specific stream power; however, the reach average shear stress is often used, which is not an accurate estimate of the force acting on individual grains.

### Incipient motion

Several methods have been proposed to quantify critical specific stream power ( $\omega_c$ ) for incipient motion, but most require additional data that are not easily quantified at the catchment scale. For example, the Bagnold (1980) formula for  $\omega_c$  is dependent on flow depth to account for flow resistance (via relative roughness):

$$\omega_c = 5.75 * \left( \frac{g}{\rho} \right)^{0.5} [(\rho_s - \rho) * D_{50} * 0.04]^{3/2} * \log \left( \frac{12h}{D_{50}} \right) \quad (3)$$

where  $\omega_c$  is in units of  $\text{kg m}^{-1} \text{s}^{-1}$ . Note that the units here are different from in Equation (1) because Bagnold divided  $\omega$  by gravitational acceleration to yield the same units as bedload transport rate (Ferguson, 2005; Parker et al., 2011).

Camenen (2012) and Ferguson (2012) used theoretical approaches to develop equations to predict dimensionless critical specific stream power ( $\omega_{c*}$ ) as a function of grain size and grain sorting ( $D_{84}/D_{50}$ ), respectively. Dimensionless specific stream power is defined as:

$$\omega_* = \frac{\omega}{\rho((s-1)gD_{50})^{3/2}} \quad (4)$$

where here,  $\omega$  is in units of  $\text{N m}^{-1} \text{s}^{-1}$  (or  $\text{W m}^{-2}$ ).

Because grain size and grain sorting are both correlated with channel slope, Camenen and Ferguson’s equations both predict a non-linear relationship between slope and  $\omega_{c*}$ . But, these equations predict  $\omega_{c*}$  varies by only a factor of ~1.5 for a wide range of slopes (0.02–30%). Eaton and Church (2011) proposed another method for determining  $\omega_{c*}$  using Shield’s parameter and a flow resistance term. Since both parameters vary with slope, this approach also has an inherent slope dependence.

Parker et al. (2011) collected incipient motion data from field and flume studies and showed that dimensionless critical specific stream power ( $\omega_{c*}$ ) was not correlated with slope and had a mean value of ~0.1. Using this estimate,  $\omega_c$  can be calculated from Equation (4) using only grain size.

The Parker et al. (2011) method for quantifying  $\omega_c$  is attractive in its simplicity, but other approaches may be more robust (Bagnold, 1980; Eaton and Church, 2011; Camenen, 2012; Ferguson, 2012). We compare the accuracy of all these methods to determine which is most appropriate for our new sediment transport equations.

## Sediment transport equations

Bagnold (1966) defined stream power as the available power supply in a stream and used it to derive a theoretical bedload transport relationship (Bagnold, 1973). Unfortunately, this equation failed to match field observations, leading Bagnold to develop an empirical version (Bagnold, 1977, 1980):

$$\frac{q_b}{q_{b,ref}} = \frac{s}{s-1} \left[ \frac{\omega - \omega_c}{(\omega - \omega_c)_{ref}} \right]^{3/2} \left( \frac{h}{h_{ref}} \right)^{-2/3} \left( \frac{D_{50}}{D_{50,ref}} \right)^{-1/2}$$

$$q_{b,ref} = 0.1 \text{ kg m}^{-1}\text{s}^{-1}, (\omega - \omega_c)_{ref} = 0.5 \text{ kg m}^{-1}\text{s}^{-1}$$

$$h_{ref} = 0.1 \text{ m}, D_{50,ref} = 1.1E - 3 \text{ m}$$
(5)

where  $q_b$  is the unit bedload transport rate ( $\text{kg m}^{-1}\text{s}^{-1}$  dry mass), and  $\omega$  and  $\omega_c$  are specific and critical specific stream power, respectively (also in  $\text{kg m}^{-1}\text{s}^{-1}$ ). The term  $\frac{s}{s-1}$  was added to convert from immersed to dry mass (Gomez and Church, 1989). The subscript *ref* refers to reference values which Bagnold used to make this empirical equation dimensionless.

Martin and Church (2000) made this equation dimensionally consistent without relying on reference values:

$$q_b = [\omega - \omega_c]^{3/2} \frac{D_{50}^{1/4}}{h} \frac{1}{\rho_r^{1/2} g^{1/4}}$$
(6)

where  $\rho_r$  is submerged sediment density ( $\rho_s - \rho$ ). They determined that this equation outperformed all other variations they examined, including Bagnold's 1980 version. A more recent analysis using a comprehensive bedload transport dataset resulted in a purely empirical equation using only dimensionless specific stream power (Parker, 2010; Parker et al., 2012):

$$q_{b*} = \begin{cases} 100\omega_*^6 & \text{for } \omega_* < 0.25 \\ 0.2\omega_*^{1.5} & \text{for } \omega_* \geq 0.25 \end{cases}$$
(7)

where  $q_{b*}$  is dimensionless unit bedload transport rate (analogous to Einstein's sediment transport parameter but with different units of bedload transport):

$$q_{b*} = \frac{q_b}{\rho((s-1)gD_{50})^{3/2}}$$
(8)

where  $q_b$  is in units of  $\text{N m}^{-1}\text{s}^{-1}$  (submerged weight of sediment). Another empirical relationship relates dimensionless specific stream power to a new dimensionless transport parameter,  $E^*$  (Eaton and Church, 2011):

$$E^* = \left[ 0.92 - 0.25 \left[ \frac{\omega_{c*}}{\omega_*} \right]^{1/2} \right]^9$$
(9)

where  $\omega_{c*}$  can be calculated using the Shield's parameter and a flow roughness variable (see Appendix, Equations (A1)–(A2)). The dimensionless transport parameter is a function of transport rate, unit discharge, and slope:

$$E^* = \frac{(s-1)q_b}{qs}$$
(10)

where  $q_b$  is in units of  $\text{m}^3 \text{m}^{-1}\text{s}^{-1}$  and  $q$  is unit discharge ( $Q/w; \text{m}^2 \text{s}^{-1}$ ).

Williams (1970) used flume data – accounting for the effects of wall roughness – to show that, all else being equal, sediment

transport rate increased as depth decreased. Expanding this to field data, Bagnold (1977) confirmed that bedload transport rate was inversely related to relative roughness ( $h/D_{50}$ ). While the Bagnold (1980) transport equation did not contain relative roughness explicitly, sediment transport rate is inversely related to flow depth (Equation (5)).

Since the purpose of simplifying the Bagnold sediment transport relationship is to eliminate the depth term without losing significant predictive power, we selected another variable that is proportional to depth – unit discharge ( $q = Q/w$ ). From continuity, we can show that flow depth is related to unit discharge:

$$Q = whV$$

$$\frac{Q}{wV} = \frac{q}{V} = h$$
(11)

where  $V$  is flow velocity ( $\text{m s}^{-1}$ ), and  $q$  is unit discharge ( $\text{m}^2 \text{s}^{-1}$ ). Depth and unit discharge are only equal at constant velocity. Also, depth is influenced by roughness and we neglect roughness effects on sediment transport by using unit discharge instead. Despite this simplification, we will show that using  $q$  in place of depth does not substantially reduce the accuracy of our sediment transport equations. In this paper, we developed and tested new bedload and total load equations with a similar form to Bagnold (1980) and Martin and Church (2000), but using unit discharge in place of depth. These equations have the following structure:

$$q_s = a[\omega - \omega_c]^b D_s^c q^d$$
(12)

where  $a$ ,  $b$ ,  $c$ , and  $d$  are empirically fitted values.

## Methods

### Data collection

We collected flume data of incipient grain motion from the literature, including sources used by others in critical stream power analyses (Table I; Parker et al., 2011; Camenen, 2012; Ferguson, 2012). The definition of incipient motion varied among these datasets which may impact direct comparison among sources. The full incipient motion database is in Table S1, Supplementary information.

Sources of flume and field bedload transport data are summarized in Table II. When testing bedload transport equations, it is important to use data at equilibrium transport (Gomez and Church, 1989). Equilibrium transport assumes steady flow and constant sediment characteristics but may be practically achieved if the material in transport is representative of the material in the streambed. The data compiled by Gomez and Church (1988) meet the equilibrium transport standard by ensuring the bedload  $D_{50}$  is within one phi unit of the subsurface bed  $D_{50}$  (where phi =  $-\log_2 D_s$ ). In addition, Gomez and Church (1988) excluded flume data if bedforms were observed, the Froude number was greater than one, or the width-depth ratio was less than 10.

Additional bedload transport data were obtained from other sources (Yang, 1979; Williams and Rosgen, 1989; Bravo-Espinosa, 1999; Almedeij, 2002; King et al., 2004; Parker, 2010; Hinton et al., 2016). We assessed equilibrium transport conditions using two methods. If full bed material and bedload grain size distributions were available, we adjusted transport rates to include only the fraction of the bedload that was within one phi unit of the bed material  $D_{50}$  (after Parker, 2010). If these full grain size distributions were not available, we only

**Table I.** Summary of data used in the incipient motion analysis

Study	Abbr.	Type	N	Slope [m m <sup>-1</sup> ]	$\omega$ [W m <sup>-2</sup> ]	D <sub>50</sub> [mm]	Incipient method
Bathurst et al. (1987)	Bathurst	Flume	12	0.005–0.09	7.6–55.6	11.5–44.3	Extrapolating graphical relationships between water discharge and sediment discharge
Bathurst (1979) cited in Bathurst (2013)	Bathurst	2	Flume	3	0.05–0.08	5.1–35.3	8–34
Dey and Raju (2002)	Dey, Raju	Flume	33	0.0101–0.0169	1.2–4.6	4.89–9.47	Extrapolating graphical relationships between water discharge and sediment discharge
Ikeda (1983) cited in Bathurst (2013)	Ikeda	Flume	3	0.0025–0.009	2.7–4.6	6.4	All surface fractions showed movement
Johnson (1943) cited in Parker et al. (2011)	Johnson	Flume	21	0.0015–0.1	0.1–1.8	1.4–4.4	Extrapolating graphical relationships between water discharge and sediment discharge
Mizuyama (1977)	Mizuyama	Flume	12	0.01–0.2	2.1–22.4	6.4–22.5	$q_{b^*} = 0.0001$ ; extrapolated from sediment transport data <sup>1</sup>
Meyer-Peter and Müller (1948) cited in Bathurst (2013)	MPM	Flume	7	0.00275–0.0065	1.2–62	3.3–28.65	Extrapolating graphical relationships between water discharge and sediment discharge
Parker et al. (2011)	Parker	Flume	14	0.0071–0.0167	3.3–8.6	6–11.5	$q_{b^*} = 0.0001$ ; extrapolated from sediment transport data <sup>1</sup>
Prancevic and Lamb (2015) and Prancevic et al. (2014)	Prancevic	Flume	20	0.031–0.41	5.6–12.9	15	Extrapolating graphical relationships between water discharge and sediment discharge
Shvidchenko and Pender (2000) cited in Parker et al. (2011)	S.P	Flume	33	0.0019–0.0287	0.2–9.8	1.5–12	$q_{b^*} = 0.0001$ ; extrapolated from sediment transport data <sup>1</sup>
Saad (1989)	Saad	Flume	16	0.00143–0.0063	0.3–5.6	1.19–9.5	Run flume until armor layer developed, incipient motion of this layer assumed
Yang et al. (2006)	Yang	Flume	21	0.0049–0.0253	0.2–29.8	7–40	$W = 0.02$ (Taylor, 1971)
King et al. (2004)	–	Field	45	0.0005–0.057	18.3–174.4	9–186	$q_{b^*} = 0.0001$ ; extrapolated from sediment transport data <sup>1</sup>

<sup>1</sup>We performed this analysis given the full sediment transport dataset.

included data where the bedload D<sub>50</sub> was within one phi unit of the subsurface D<sub>50</sub> (after Gomez and Church, 1988).

We obtained total load transport data from Brownlie (1981). Only a subset of these data were used, consistent with Brownlie's criteria for the development of his total load equation (Brownlie, 1982). We filtered data using the following restrictions: 0.062 mm < D<sub>50</sub> < 2 mm; σ<sub>g</sub> < 5; w/h > 4; R<sub>b</sub>/D<sub>50</sub> > 100, and Q<sub>t</sub> > 10 ppm. Despite using the same criteria, we kept more data points than Brownlie (1463 compared with 999). We made sidewall corrections (Vanoni, 1975) to adjust hydraulic radius for the Ackers and White (1973), Engelund and Hansen (1967), and Brownlie (1982) total load equations. The full bedload and total load datasets are in Tables S2 and S3.

### Incipient motion analysis

We used flume and field data to examine the relationship between ω<sub>c\*</sub> and channel slope. We also assessed the accuracy of five methods for computing critical specific stream power: Bagnold (1980), Eaton and Church (2011), Parker et al. (2011), Camenen (2012), and Ferguson (2012) (see Appendix for details on these methods). Only flume data were included in this analysis because field data did not include all the inputs required by these methods.

Critical specific stream power for field data and three flume studies (Johnson, 1943; Shvidchenko and Pender, 2000; Parker et al., 2011) was computed indirectly. Dimensionless bedload transport rate ( $q_{b^*}$ , Equation (8)) was plotted versus dimensionless specific stream power ( $\omega^*$ , Equation (4)). A best fit line was computed as the bisector of the y-on-x and x-on-y least-squares regression lines using log10-transformed data. We adjusted the fitted coefficient for de-transformation bias after Ferguson (1986):

$$c_{adj} = 10^{c_{orig}} * e^{2.65s^2} \quad (13)$$

$$s^2 = \frac{1}{n-2} \sum_{i=1}^n (q_{b^*i} - q_{b^*,pred,i})^2 \quad (14)$$

where  $c_{adj}$  is the adjusted coefficient (in normal space),  $c_{orig}$  is the original (in log space),  $s^2$  is the estimated variance, and  $n$  is the total number of data points. Dimensionless critical specific stream power was calculated as the intersection of this best fit line and  $q_{b^*} = 0.0001$ , a value corresponding to incipient motion of bed particles (Parker et al., 2011; Ferguson, 2012). We used best judgment to exclude field sites with insufficient data to develop an accurate best fit or if substantial extrapolation was required to reach  $q_{b^*} = 0.0001$ .

We quantified how the uncertainty in ω<sub>c\*</sub> is translated into uncertainty in ω<sub>c</sub> for a range of grain sizes. We ran Monte Carlo simulations selecting ω<sub>c\*</sub> values from a lognormal distribution that approximated the collected flume and field data (log-mean = -2.51, log-sd = 0.40) and computed ω<sub>c</sub> using Equation (4).

### Bedload transport equation

We developed a new version of the Bagnold (1980) empirical bedload transport equation using unit discharge in place of flow depth. We first created a dimensionally consistent equation following Martin and Church (2000); however, the dimensionally consistent equation was relatively inaccurate and was therefore not included in further analysis. Instead, we developed empirical equations using a similar transport dataset to Martin and Church (2000), but using Parker et al.'s (2011) equation for ω<sub>c</sub> ( $\omega_{c^*} = 0.1$ ; Equation (4)). Only the subsurface

**Table II.** Summary of bedload transport data used in this analysis (excluding data where no transport was predicted)

Source	Type	Site/Study	N	D <sub>50</sub> [mm]	S [m m <sup>-1</sup> ]	q <sub>b</sub> [kg m <sup>-1</sup> s <sup>-1</sup> ]	ω [W m <sup>-2</sup> ]
Almedeij (2002)	Field	Goodwin Creek	92	11.7	0.0024–0.0034	0.0057–2.98	25.5–45.1
		Chippewa River at Durand	25	0.6	3e-04–4e-04	0.00386–0.11059	0.9–11.4
		Chippewa River at Pepin	18	0.5	2e-04–6e-04	0.00684–0.05307	1.3–5.3
		North Fork Toutle River	6	10	0.0032–0.0079	1.61224–5.72881	71.3–123.2
		Toutle River	13	8	0.0019–0.0055	0.14581–3.46269	17.1–412.3
		Wisconsin River	19	0.4	2e-04–5e-04	0.00479–0.13881	0.8–17.9
Bravo-Espinosa (1999)	Field	Yampa	29	0.6	5e-04–9e-04	0.00812–0.85806	1.8–39.9
		Clearwater River <sup>1</sup>	5	32	4e-04–6e-04	0.0317–0.2581	47.2–129.2
		East Fork River <sup>1</sup>	38	1.2	7.00E-04	0.0112–0.1268	3.2–15.1
		Elbow River <sup>1</sup>	19	27	0.0074	0.0385–0.9242	74.6–146.7
		Mountain Creek <sup>1</sup>	37	0.9	0.0015–0.0016	0.00467–0.0262	0.6–1.6
		Snake River <sup>1</sup>	17	32	7e-04–0.0011	0.0161–0.3103	43.5–177.1
		Tanana River <sup>1</sup>	14	7.6	5e-04–6e-04	0.0327–0.2482	13.1–27.3
		ETH: 2 <sup>1</sup>	14	1.5	0.0022–0.0029	0.0045–0.147	0.9–4.7
		ETH: 3 <sup>1</sup>	6	3.7	0.008–0.0083	0.059–0.332	4–8.8
		IIHR: 1	6	4.4	0.0042–0.0048	0.00088–0.01844	2.1–3.2
		IIHR: 2	12	3.4	0.0046–0.0095	0.00119–0.01976	1.4–2.5
		IIHR: 3	24	2.3	0.0025–0.005	5e-05–0.02315	0.7–1.4
Gomez and Church (1988)	Flume	IIHR: 4	31	1.4	0.0014–0.005	0.00062–0.01978	0.4–0.9
		IIHR: 5	10	3.6	0.0034–0.0054	0.00011–0.01724	1.5–2.9
		IIHR: 6	27	1.8	0.0018–0.005	0.00019–0.01703	0.5–1
		Ikeda <sup>1</sup>	7	6.5	0.0023–0.0052	3e-04–0.0779	3.7–9.2
		Paintal	21	2.5–22.2	0.0013–0.0091	5e-05–0.04961	0.8–25.1
		Wilcock–1.0Phi <sup>1</sup>	1	1.8	0.0011	0.00003	0.6
		Wilcock – CUNI <sup>1</sup>	2	5.3	0.0038–0.0049	0.00056–0.00096	3–4.4
		Wilcock – MUNI <sup>1</sup>	1	1.9	0.0012	0.00036	0.7
		Williams <sup>1</sup>	19	1.4	6e-04–0.0044	0.0014–0.0865	0.5–5.3
		East St. Louis Creek	10	51	0.054–0.0577	0.00038–0.0033	135.6–228.3
		Fool Creek	3	38	0.055	8e-04–0.00255	74.5–130.3
Hinton et al. (2016)	Field	Little Granite Creek	3	58	0.02	0.04268–0.04946	167.8–319.3
		Sagehen Creek	2	58	0.0095	0.01155–0.01294	112–112.3
		St. Louis Creek Site 2	1	76	0.019	0.00499	152.2
		Boise River	3	74	0.0038	0.02643–0.12124	148.6–187.8
		Bruneau River	35	34	0.0054	8e-05–0.00572	41–95.8
		Cat Spur Creek	2	27	0.0111	0.00031–0.00123	34.4–37.3
		Fourth of July Creek	3	51	0.0202	0.00028–0.00099	82.7–90.8
		Hawley Creek	2	40	0.0233	3e-05–0.00016	60–68.5
		Lolo Creek	1	68	0.0097	0.00343	174.5
		Main Fork Red River	1	59	0.0059	0.00007	105.3
		Marsh Creek	3	56	0.006	0.00027–0.00266	93.4
		South Fork Payette River	2	82.5	0.004	0.00921–0.01527	163
King et al. (2004)	Field	South Fork Salmon River	8	38	0.0025	0.00017–0.00269	63.8–104.7
		Squaw Creek (USFS)	26	27	0.024	0–0.01621	30.8–105.7
		Trapper Creek	1	76	0.0414	0.00102	149.9
		Valley Creek	8	40	0.004	5e-05–0.01489	55.2–86.3
		Black River	7	0.5	1e-04–3e-04	0.01213–0.04134	0.4–3.4
		Chippewa River near Caryville	6	4.4	2e-04–3e-04	0.00028–0.00874	3.2–7.7
		Chulitna River near Talkeetna	36	10.6	4e-04–0.0026	0.00662–0.5567	8–253.2
		Muddy Creek	21	0.8	0.0012	0.00018–0.10115	0.5–3.9
		Pony Creek	13	2.1	0.005–0.006	1e-05–0.00111	1–3
		Rich Creek	1	54.4	0.039	0.00415	96.1
		Susitna River at Sunshine	23	39.4	0.0014–0.0024	0.0022–0.21151	59–214
		Susitna River near Talkeetna	1	53.5	0.0016	0.0083	86.3
Williams and Rosgen (1989)	Field	Tanana River at Fairbanks	30	2.4	4e-04–0.0041	0.00232–0.18377	10.6–157.9
		Trail Creek	13	2.5	0.018	7e-05–0.01548	6.3–28.8
		Niobrara River	25	3.00E–01	0.0011–0.0018	0.07127–1.05258	3.2–12.7
		Middle Loup River	15	3.00E–01	9e-04–0.0015	0.08205–0.42839	2.5–4.1
		Mississippi River	25	0.2–0.8	0–1e-04	0.00807–2.08758	1.9–20.5
		Rio Grande A	42	0.2–0.4	7e-04–9e-04	0.03777–5.0349	2–26.4
		Gilbert	630	0.3–1.7	0.0013–0.0296	0.00218–1.06545	0.2–11.3
		Guy	315	0.2–0.9	1e-04–0.0193	1e-05–12.00662	0.1–60.8
		Kennedy	41	0.2–0.5	0.0017–0.0272	0.00722–2.52413	0.6–14.4
		Nomicos	12	0.2	0.002–0.0039	0.00348–0.21597	0.3–1.5
		Rio Grande B	31	0.1–0.2	1e-04–0.0043	0.00485–7.14127	0.4–23.2
Yang (1979)	Flume	Shvidchenko and Pender	146	1.5–12	0.0026–0.0287	2e-05–0.02019	0.4–11.4
		Shvidchenko	73	2.6–6.4	0.0041–0.0141	5e-05–0.03034	0.9–6.2

(Continues)

**Table 2.** (Continued)

Source	Type	Site/Study	N	D <sub>50</sub> [mm]	S [m m <sup>-1</sup> ]	q <sub>b</sub> [kg m <sup>-1</sup> s <sup>-1</sup> ]	ω [W m <sup>-2</sup> ]
	Stein		42	0.4	6e-04–0.0108	0.00771–4.74627	0.7–28.9
	Vanoni and Brooks		14	0.1	7e-04–0.0028	0.00041–0.09522	0.2–0.9
	Wilcock		23	5.3–12.2	0.007–0.0204	0.00091–0.50444	5.3–24.6

<sup>1</sup>Data used to fit Equation (15).

D<sub>50</sub> was available for these data, which may alter the empirical fits. We used multiple linear regression of the log10-transformed data, with coefficient bias correction after Ferguson (1986).

The initial fitted exponents were very close to rational fractions. We fixed these exponents and allowed only the coefficient to vary yielding a new version of the Bagnold (1980) equation but with unit discharge in place of flow depth:

$$q_b = a[\omega - \omega_c]^{3/2} D_s^{-1/2} q^{-1/2} \quad (15)$$

where the coefficient  $a$  is 0.0044 if  $\omega$  and  $\omega_c$  are in units of kg m<sup>-1</sup> s<sup>-1</sup> (after Bagnold's original definition) but is 1.43E-4 if  $\omega$  and  $\omega_c$  are in units of W m<sup>-2</sup>.

Despite the strong physical basis for including a threshold of motion (e.g. critical specific stream power) in bedload transport equations, inaccuracies in  $\omega_c$  can cause transport equations to predict no sediment movement when movement occurs. To avoid this issue, we developed an alternative equation with no critical specific stream power. This equation, however, performed poorly (root-mean-square error (RMSE)=2.81 and R<sup>2</sup>=0.66). In this framework, the Parker (2010) bedload equation is a more accurate option that does not rely on critical specific stream power.

We used the full bedload transport dataset to test our new empirical equation against four existing stream power based formulae: Bagnold (1980), Martin and Church (2000), Parker (2010), and Eaton and Church (2011). We quantified equation accuracy using four metrics: RMSE (Equation (16)), root-mean-square-logarithmic-error (RMSLE; Equation (17)), Theil's (1958) measure of association ( $U$ ; Equation (18); Smith and Rose, 1995), and the adjusted coefficient of determination using log10-transformed data (R<sup>2</sup>; Equation (19)).

$$\text{RMSE} = \sqrt{\frac{1}{n} \sum_{i=1}^n (q_{b,i} - q_{b,pred,i})^2} \quad (16)$$

$$\text{RMSLE} = \sqrt{\frac{1}{n} \sum_{i=1}^n (\log q_{b,i} - \log q_{b,pred,i})^2} \quad (17)$$

$$U = \frac{\sqrt{\frac{1}{n} \sum_{i=1}^n (q_{b,i} - q_{b,pred,i})^2}}{\sqrt{\frac{1}{n} \sum_{i=1}^n q_{b,i}^2} + \sqrt{\frac{1}{n} \sum_{i=1}^n q_{b,pred,i}^2}} \quad (18)$$

$$R^2 = 1 - \frac{1 - \frac{\sum_{i=1}^n (\log q_{b,i} - \log q_{b,pred,i})^2}{\sum_{i=1}^n (\log q_{b,i} - \log \text{mean}(q_{b,i}))^2} * (n - 1)}{(n - p - 1)} \quad (19)$$

where  $n$  is the sample size and  $p$  is the number of fitted model parameters.

Each of these error measures has benefits and drawbacks and it is useful to examine them collectively to assess model fit. RMSE is the average error across all observations and is in the same units as sediment transport (kg m<sup>-1</sup> s<sup>-1</sup> or ppm); however, high transport values have a larger influence on estimating

model accuracy due to the orders of magnitude variation in transport data. We therefore used log-transformed data for the RMSLE and adjusted R<sup>2</sup> value to obtain a more balanced error estimate. Similar to R<sup>2</sup>, Theil's measure of association estimates relative error (on a 0 to 1 scale), but it also accounts for how close predictions are to the 1:1 line (Smith and Rose, 1995). Smaller values indicate a better fit for RMSE, RMSLE, and  $U$ , while higher values do for R<sup>2</sup>. We only used data where all equations predicted transport to allow direct comparisons between formulae.

We used a density-based sensitivity analysis (Plischke et al., 2013) to assess the relative importance of equation variables on calculated sediment transport rates. Briefly, conditional probability density functions (pdfs) for each input variable are compared with the full output pdf. Larger differences between the conditional and full pdfs indicate larger parameter influence on model output. We estimated input variable distributions based on observed distributions in the collected bedload transport data (Table III).

## Total load transport equation

Because the dimensionally consistent bedload transport equation failed to predict observed transport rates, we opted for a purely empirical approach to develop a total load equation. The total load database was randomly split into a 'training' set ( $N=731$ ) and a 'testing' set ( $N=732$ ). We used the same parameter set as the bedload formula and fitted the model using multiple linear regression on the log10 transformed training set, with bias correction. Like the empirical bedload equation, fitted exponents were close to rational fractions. Fixing these exponents and allowing only the coefficient to vary yielded:

$$Q_t = a[\omega - \omega_c]^{3/2} D_s^{-1} q^{-5/6} \quad (20)$$

where  $Q_t$  is the total sediment load (ppm). The coefficient  $a$  is 0.6568 if  $\omega$  and  $\omega_c$  are in units of kg m<sup>-1</sup> s<sup>-1</sup> but is 0.0214 if  $\omega$  and  $\omega_c$  are in units of W m<sup>-2</sup>.

We used the testing dataset to compare Equation (20) with three existing total load equations: Ackers and White (1973), Engelund and Hansen (1967), and Brownlie (1982) (see Appendix for formulae). We chose the Ackers and White and Engelund and Hansen equations because they performed best among the equations examined by Brownlie (1982). We also performed a sensitivity analysis of Equation (20). We estimated input distributions based on observed distributions in the collected total load transport data (Table IV). Table V shows ranges of input values for which the bedload and total load equations were tested. All analyses were done in R version 3.2.5 (R Core Team, 2016).

## Incision modeling

We tested the applicability of our bedload transport relationship by modeling channel incision using the flume experiment of Ashida and Michie (1971). We did not use our total load

**Table III.** Summary of distributions used in the bedload sensitivity analysis

Variable	Distribution	Min	Max
$D_{50}$ [m]	Log-Uniform	0.0001	0.2
$\omega_c^*$	Lognormal (mean = -2.4, sd = 0.46)	0.03	0.3
Slope [ $m m^{-1}$ ]	Lognormal (mean = -5.6, sd = 1.83)	5e-5	0.06
Discharge [ $m^3 s^{-1}$ ]	Lognormal (mean = 1.45, sd = 3.50)	0.008	6000
Width [m]	Lognormal (mean = 2.2, sd = 1.96)	0.2	500

**Table IV.** Summary of distributions used in the total load sensitivity analysis

Variable	Distribution	Min	Max
$D_{50}$ [m]	Lognormal (mean = -7.9, sd = 0.52)	0.00008	0.002
$\omega_c^*$	Lognormal (mean = -2.4, sd = 0.46)	0.03	0.3
Slope [ $m m^{-1}$ ]	Lognormal (mean = -8.4, sd = 1.20)	9e-6	0.02
Discharge [ $m^3 s^{-1}$ ]	Lognormal (mean = 4.4, sd = 3.33)	0.002	30000
Width [m]	Lognormal (mean = 6.0, sd = 1.34)	0.3	1200

equation because the grain sizes in this experiment were outside the range of grain sizes used to fit this equation. We used data from run 6 of their experiments from a 20 m long, 0.8 m wide rectangular flume with an initial bed slope of 0.01 and a constant discharge of  $0.0314 m^3 s^{-1}$ . They used a graded sediment mixture with a mean of 2.47 mm and a standard deviation of 3.73 mm. The bed slope was initially stable and the sediment feed was cut off at the start of the experiment. The downstream bed elevation was controlled by a weir.

While our goal is to develop sediment transport equations for application throughout a river network, we chose to test our bedload equation using a flume dataset for two reasons. First, there are limited field data describing network-scale channel incision. Second, flume studies generally have more accurate data and simpler conditions (e.g. constant discharge and fixed width) which allowed us to examine the uncertainty in our bedload transport equation while minimizing confounding factors. Ashida and Michiue's data have the added benefit of being used to test a complex morphodynamic channel degradation model: CONservational Channel Evolution and Pollutant Transport System (CONCEPTS) (Langendoen and Alonso, 2008). We compared our incision model output with the experimental results and the CONCEPTS results.

Ashida and Michiue's (1971) flume incised while the bed armored, which controlled the extent and rate of channel incision. To account for this armoring process, we modeled sediment transport by grain size fraction. Since no stream power based hiding function exists, we adjusted each

representative grain size to calculate  $\omega_c$  (Garbrecht et al., 1995; Langendoen and Alonso, 2008):

$$D_{c,k} = D_k \left( \frac{D_m}{D_k} \right)^\eta \quad (21)$$

where  $D_{c,k}$  is the adjusted critical grain size of size class  $k$ ,  $D_k$  is the actual grain size,  $D_m$  is the geometric mean grain size of the bed, and  $\eta$  is a hiding coefficient. Following Langendoen and Alonso (2008), we set  $\eta$  equal to 0.7. Channel incision was modeled using the Exner equation:

$$\frac{\partial z}{\partial t} = -\frac{1}{1-\lambda} \frac{\partial q_s}{\partial x} \quad (22)$$

where  $z$  is the bed elevation,  $q_s$  is the volumetric sediment transport rate per unit width, and  $\lambda$  is the bed porosity. Numerically, the sediment transport rate was estimated using the Quick scheme (Hirsch, 2007):

$$q_{s,i+1/2} = q_{s,i} + \frac{1}{8} (q_{s,i} - q_{s,i-1}) + \frac{3}{8} (q_{s,i+1} - q_{s,i}) \quad (23)$$

where the subscript  $i$  refers to the cross-section (increasing in the downstream direction) and the value of  $\frac{\partial q_s}{\partial x}$  from Equation (22) is calculated as:

$$\frac{\partial q_s}{\partial x} = q_{s,i+1/2} - q_{s,i-1/2} \quad (24)$$

The change in the bed grain size distribution was calculated using the following (Langendoen and Alonso, 2008):

$$\frac{\partial p_{s,k} A_s}{\partial t} = (1-\lambda) w \frac{\partial z_k}{\partial t} + p_{sub,k} w \left( \frac{\partial z}{\partial t} - \frac{\partial \delta_s}{\partial t} \right) \quad (25)$$

where  $p_{s,k}$  is the proportion of the bed surface for the  $k$ th grain size,  $A_s$  is the cross-sectional area of the surface layer,  $\frac{\partial z_k}{\partial t}$  is the bed elevation change from the  $k$ th grain size,  $p_{sub,k}$  is the proportion of the subsurface for the  $k$ th grain size,  $\frac{\partial \delta_s}{\partial t}$  is the total bed elevation change, and  $\frac{\partial \delta_s}{\partial t}$  is the change in the surface layer thickness with time (assumed to be zero). The model was run for 100 hours with  $\Delta x = 1$  m,  $\Delta t = 20$  s, and  $\lambda = 0.4$ .

We incorporated uncertainty in the bedload equation into our incision model. We varied the equation coefficient and exponents uniformly across their 95% confidence intervals estimated as part of the regression fit. We ran the incision model 1000 times, giving a range of potential channel incision results.

## Results

### Incipient motion

Figure 1 shows  $\omega_c^*$  plotted versus slope for flume (1(a)) and field (1(b)) data. Lines show calculated values of  $\omega_c^*$  using the Camenen (2012) and Ferguson (2012) formulae. Dimensionless critical specific stream power is weakly correlated with slope

**Table V.** Ranges of values for which the new bedload (Equation (15)) and total load (Equation (20)) equations were tested

	$S$ [ $m m^{-1}$ ]	$Q$ [ $m^3 s^{-1}$ ]	$W$ [m]	$D_{50}$ [mm]	$q$ [ $m^2 s^{-1}$ ]	$\omega$ [ $W m^{-2}$ ]	Transport Rate
Bedload	4.28E-5–5.77E-2	3E-4–13,248	0.13–532	0.137–186	0.001–24.9	0.092–412	$7e-9$ – $12 kg m^{-1} s^{-1}$
Total load	9.6E-6–1.7E-2	2E-3–28,825	0.27–1,110	0.085–1.5	0.005–40	0.2–161	11–47,300 ppm

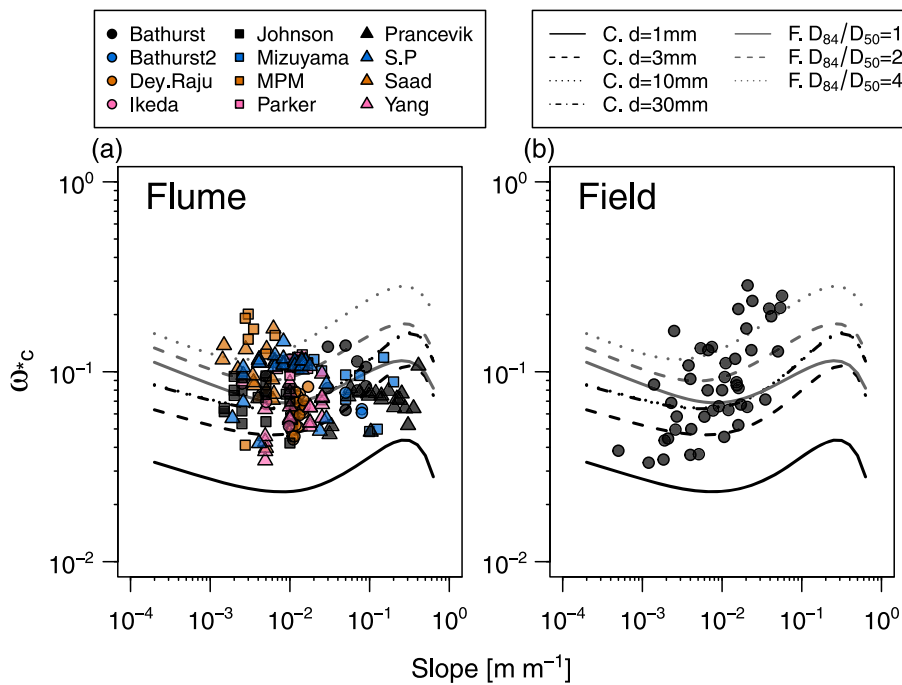


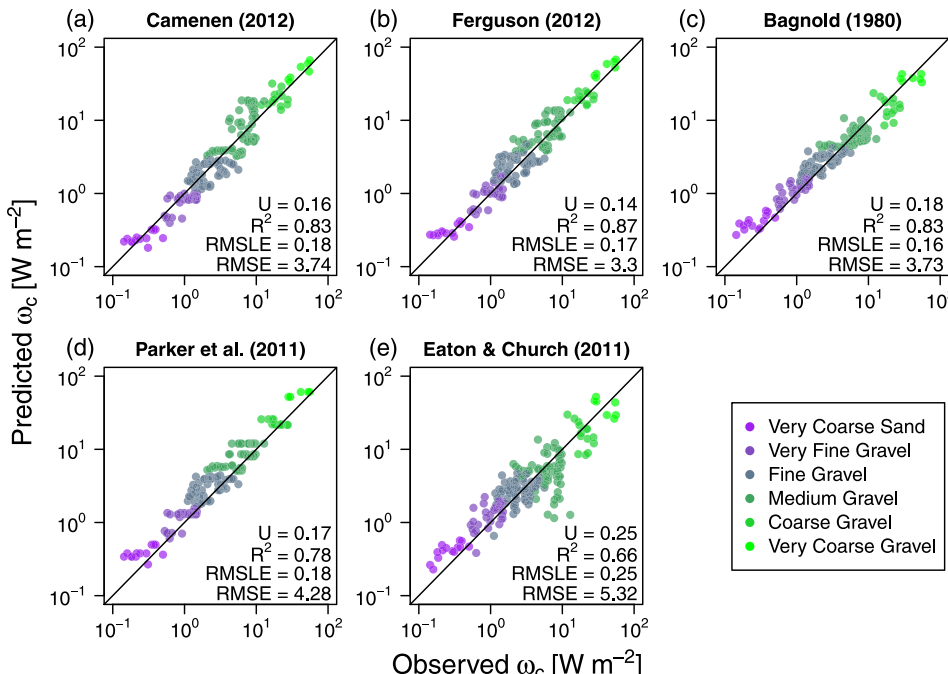
**Figure 1.** Relationships between dimensionless critical specific stream power ( $\omega_c^*$ ) and channel slope for flume (a) and field (b) data. Lines correspond to theoretical relationships based on the models of Camenen (2012) (C.) and Ferguson (2012) (F.). [Colour figure can be viewed at [wileyonlinelibrary.com](http://wileyonlinelibrary.com)]

for flume data but shows a significant positive correlation with slope for field data. Specifically, Spearman's rank-based correlation coefficient ( $\rho$ ) for flume data is negative, but insignificant at the  $\alpha=0.05$  confidence level ( $\rho=-0.14$ ;  $p=0.06$ ). Of all the flume studies, only Dey and Raju (2002) and Yang et al. (2006) show a significant correlation between  $\omega_c^*$  and slope ( $\rho=0.63$ ;  $p<1E-4$  and  $\rho=0.56$ ;  $p=0.008$ , respectively). Field data, however, show a significant positive correlation with slope ( $\rho=0.63$ ;  $p<1E-5$ ). Combined, the field and flume data are not correlated with slope ( $\rho=0.03$ ;  $p=0.63$ ). We found  $\omega_c^*$  values for flume ( $0.085 \pm 0.030$ ; mean  $\pm$  SD) and field data

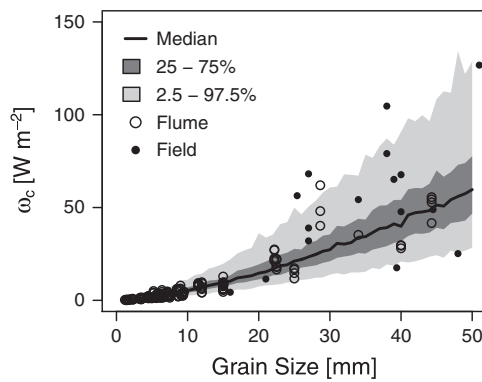
( $0.10 \pm 0.065$ ), similar to the average of 0.1 found by Parker et al. (2011), although some of the same data in Parker et al.'s dataset are included in our analysis.

Figure 2 shows observed values of  $\omega_c$  versus values predicted using the methods of Camenen (2012), Ferguson (2012), Bagnold (1980), Parker et al. (2011), and Eaton and Church (2011). The first three methods were slightly more accurate than the latter two, although all approaches show similar levels of error.

Figure 3 shows how uncertainty in  $\omega_c$  values calculated using Equation (4) and the observed distribution of  $\omega_c^*$  varies with grain



**Figure 2.** Predicted versus observed critical specific stream power for collected flume data using five different approaches. [Colour figure can be viewed at [wileyonlinelibrary.com](http://wileyonlinelibrary.com)]



**Figure 3.** Uncertainty in critical specific stream power ( $\omega_c$ ) with grain size based on simulations using the observed distribution of  $\omega_{c^*}$ . Observed data points are also shown.

size. While this uncertainty may be large for grain sizes greater than ~20 mm, uncertainty bounds are substantially smaller for finer grain sizes (95% confidence interval  $\sim 30 \text{ W m}^{-2}$  for 20 mm gravel but  $\sim 0.3 \text{ W m}^{-2}$  for 1 mm sand).

### Bedload transport equation

Figure 4 compares predicted versus observed bedload transport rates for our new bedload equation (Equation (15)) and the four established alternatives. The Bagnold (1980) empirical bedload transport equation performed best, followed by our empirical equation (Equation (15)) and the Parker (2010) equation. The Eaton and Church (2011) and Martin and Church (2000) equations were generally the least accurate. In all cases, we used the Parker et al. (2011) approach for estimating critical specific stream power ( $\omega_{c^*} = 0.1$ , Equation (4)) since our analysis suggests it is as accurate as other, more complicated alternatives. Equations with a critical specific stream power term (Bagnold, Martin and Church, and Equation (15)) predicted no motion for ~23% of the database, i.e. yielded a calculated transport

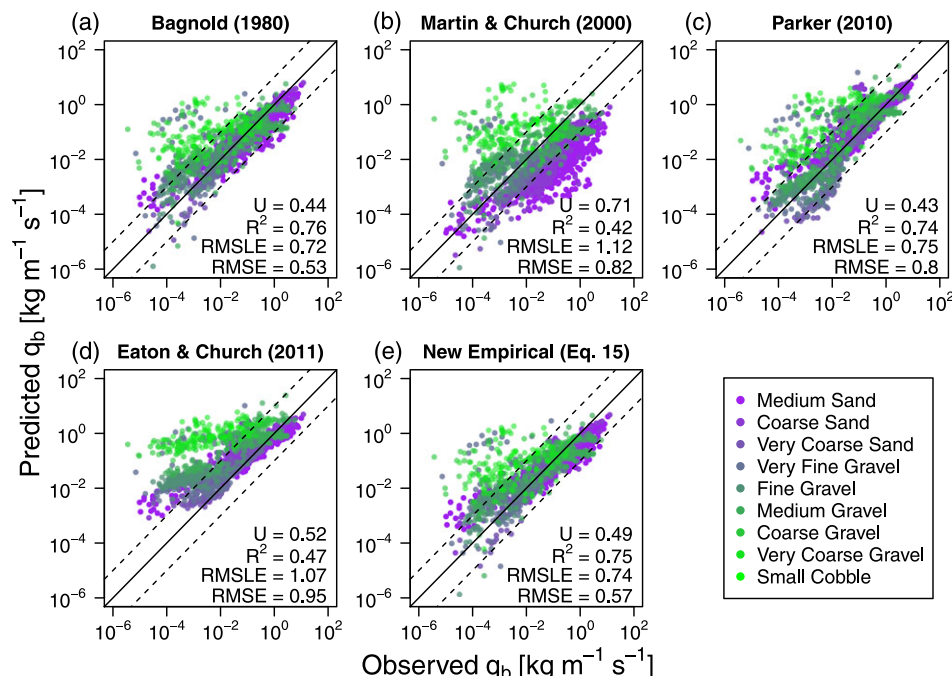


**Figure 4.** Predicted vs observed bedload transport rates for the five equations examined. The solid line is the line of perfect agreement and the dashed lines show  $\pm$  one order of magnitude. [Colour figure can be viewed at [wileyonlinelibrary.com](http://wileyonlinelibrary.com)]

rate of zero for sites with observed bedload transport. For consistency, we included only data points where all equations predicted transport. Testing with the full dataset (including zero transport predictions), did not change relative equation accuracy (RMSE decreased slightly for all equations and  $U$  was unchanged).

Figure 5 presents the results of the sensitivity analysis of Equation (15). These results suggest that discharge and slope have the largest influence on transport rates, while channel width, grain size, and  $\omega_{c^*}$  have only minor effects. This analysis, however, does not account for the threshold effect of  $\omega_{c^*}$  on determining whether transport is predicted; thus, this variable may be more important than the sensitivity results indicate.

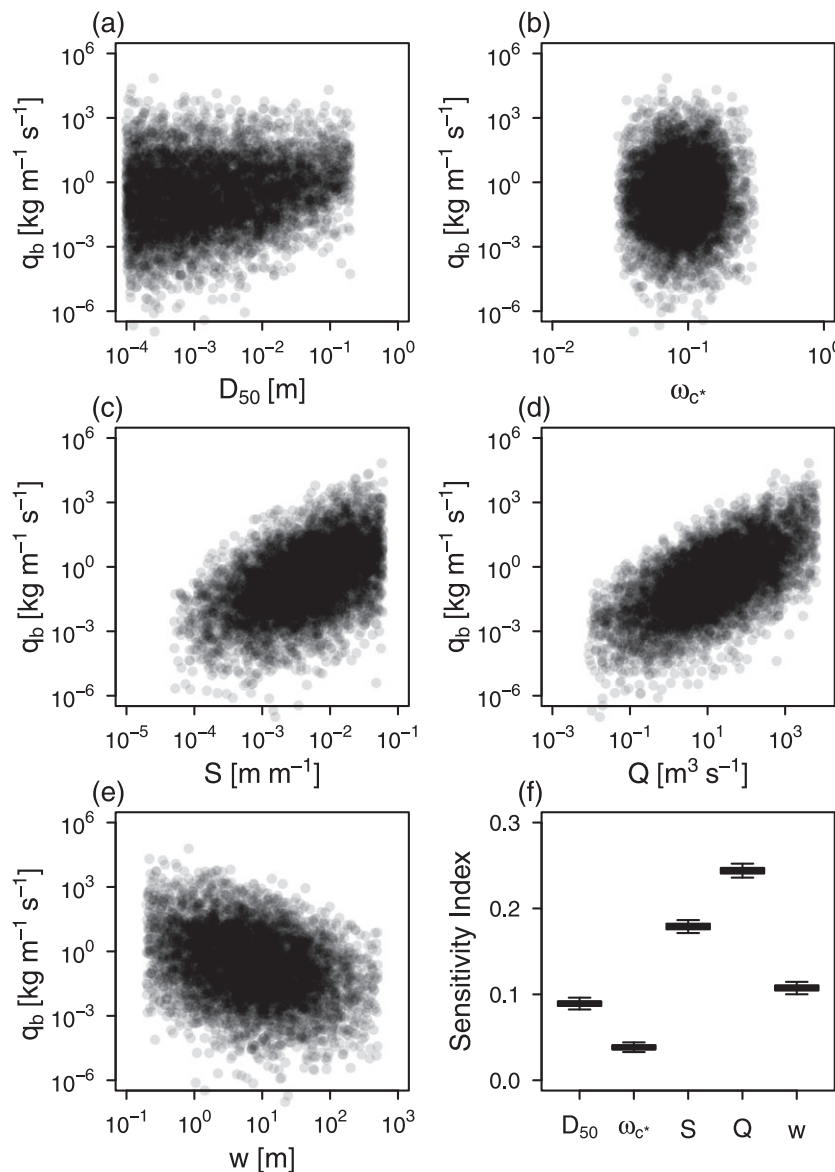
### Total load transport equation

Figure 6 compares predicted versus observed total load transport rates for Equation (20) and three commonly used total load formulae. The new equation is as accurate as these alternatives. Equation (20) is more parsimonious than Brownlie's (1982) and Ackers and White (1973), and of similar complexity to Engelund and Hansen (1967). Most importantly, Equation (20) relies on an easily quantified set of input variables, unlike the other equations which all require velocity and hydraulic radius.

Figure 7 shows the results of the sensitivity analysis of Equation (20). We converted total load transport rates from ppm to  $\text{kg m}^{-1} \text{s}^{-1}$  for this analysis to allow direct comparison with the bedload equation. The results show that discharge and slope are the most important variables, while width, grain size, and  $\omega_{c^*}$  have only a small effect.

### Incision modeling

Figure 8 shows the results of the incision modeling using our new bedload equation. We included modeled and observed erosion depth over time for three different cross-sections (8a), the modeled change in longitudinal profile (8b), and modeled



**Figure 5.** Scatterplots show simple correlation between simulated bedload transport rates and each of the five equation variables ( $N=6550$ ). Boxplot displays results of the formal sensitivity analysis of Equation (15) with bias-corrected values and uncertainty bounds based on bootstrapping with 1000 replicates.

and observed changes in bed grain size distribution for two cross-sections (8c–d). Using our new bedload equation, our incision model agrees well ( $\text{RMSE}=0.025 \text{ m}$ ) with Ashida and Michiue's (1971) experimental data and matches the incision rate more closely than the CONCEPTS results ( $\text{RMSE}=0.028 \text{ m}$ ). Uncertainty bands from the Monte Carlo analysis are shown for the erosion depth results (Figure 8(a)). Generally, there is significant uncertainty in the incision rate but much less in the predicted final erosion depth. Total uncertainty, however, may be greater in systems that do not rapidly adjust to a new stable state (in this case an armored bed) as error in incision rates will continue to propagate.

## Discussion

### Incipient motion

The Parker et al. (2011) approach to calculating critical specific stream power ( $\omega_{c^*}=0.1$ ) has similar accuracy to more complicated and data demanding equations, despite its simplicity (Figure 2). Furthermore, their method is the only one that does

not rely on flow depth or some measure of roughness. Assuming a constant value of  $\omega_{c^*}$  (or more realistically, a distribution of values) allows  $\omega_c$  to be calculated using only grain size.

We found that  $\omega_{c^*}$  is not strongly correlated with slope in the flume dataset consistent with the findings of other studies (Parker et al., 2011; Ferguson, 2012). The difference between field and flume data could result from the larger grain sizes in field sites (mean diameter of 67 mm versus 10 mm for flume data). In addition, steeper slopes in the field data may be associated with greater channel roughness, potentially leading to a correlation between  $\omega_{c^*}$  and slope. Finally, the field  $\omega_{c^*}$  values were all computed indirectly which could lead to greater uncertainty in these values compared with the flume data. Despite the apparent relationship between  $\omega_{c^*}$  and slope for field data, the Parker et al. (2011) model still had relatively low error rates for these data ( $\text{RMSE}=0.26$ ,  $U=0.26$ ).

### Sediment transport equations

The new empirical bedload (Equation (15)) and total load (Equation (20)) transport equations based on unit discharge

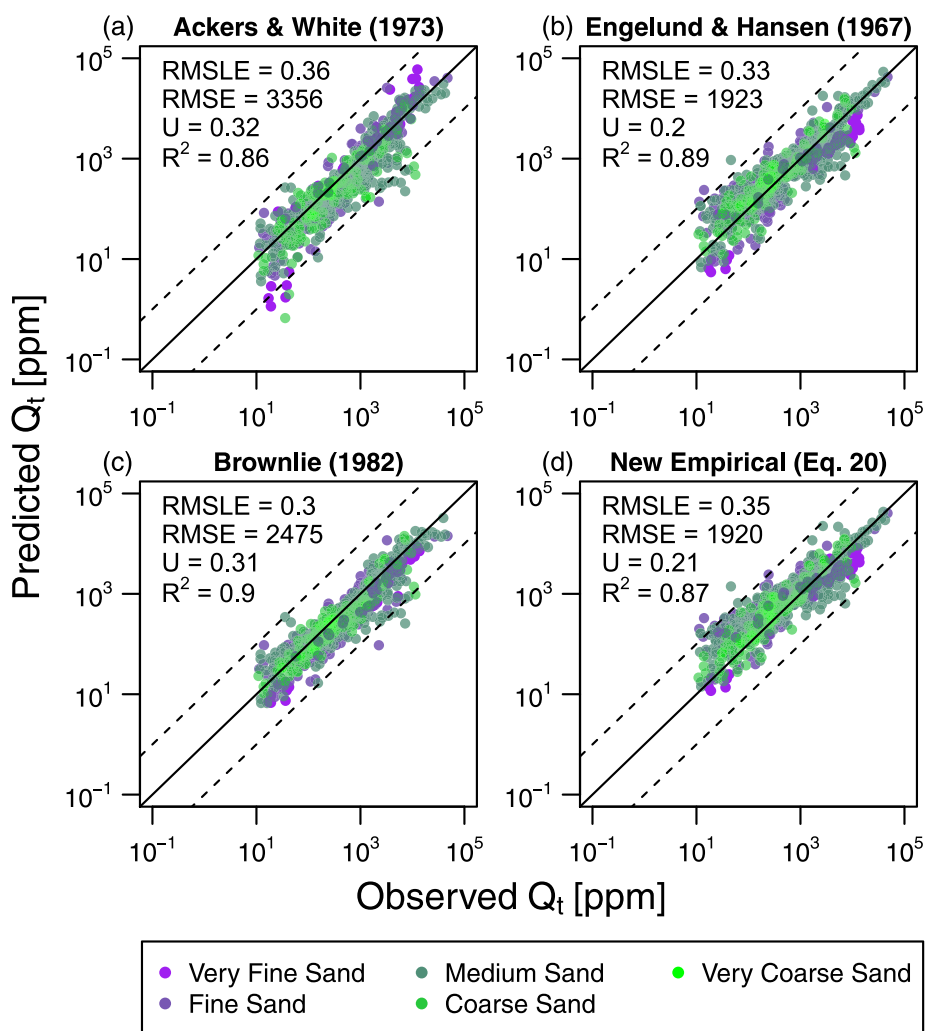


**Figure 6.** Predicted vs observed total transport rates for the four equations examined. [Colour figure can be viewed at [wileyonlinelibrary.com](http://wileyonlinelibrary.com)]

instead of flow depth have similar accuracy to more established formulae (Figures 4 and 6). The new bedload equation (Equation (15)) is nearly as accurate as the Bagnold (1980) empirical relationship and performs slightly better than other alternatives (Martin and Church, 2000; Parker, 2010; Eaton and Church, 2011). Others have shown that the Bagnold (1980) equation and Martin and Church's version tend to underpredict transport rates (Martin, 2003; Martin and Ham, 2005), although they can overpredict rates in coarser bed streams (Vázquez-Tarrío and Menéndez-Duarte, 2015). Our analysis also showed the Martin and Church (2000) equation underpredicted transport rates for finer grain sizes while all equations overpredicted rates for coarse sediment.

Differences in equation accuracy may be tied to differences in structure. For example, the equations have different relationships between bedload transport rate and median bed grain size. The Bagnold (1980) formula and the new empirical equation (Equation (15)) both have a negative exponent for grain size ( $-1/2$ ) while the Martin and Church (2000) equation has a positive exponent ( $1/4$ ). Due to the hidden positive correlation between  $\omega_c$  and grain size, however, the net relationship between transport rate and grain size is positive for all equations. The former equations perform significantly better than the latter, although this cannot be attributed solely to grain size scaling.

Our new bedload equation is simple but – like all empirical sediment transport formulae – fails to account for some processes important in bedload transport. For example,

size segregation on the channel bed can significantly affect transport rates (Frey and Church, 2011). Our bedload formula can be used to model transport by grain size, using a hiding function to adjust  $\omega_c$  – as in the incision modeling performed in this study (Equation (21)); however, it does not account for kinetic sorting mechanisms which may be a significant control on bedload transport and bed stability (Bacchi et al., 2014).

Given their simplicity, the Parker (2010) and Eaton and Church (2011) equations are also suitable for network scale application. The Parker (2010) equation, however, has no incipient motion criterion, which may be beneficial or detrimental depending on the situation. The situations in which it is beneficial to include a critical stream power (or shear stress) criterion in sediment transport modeling are not well defined, but Equation (15) and the Parker (2010) equation are two viable alternatives that can be applied when including this term may or may not be desirable. In addition, our new total load and bedload equations have the same structure and can be used in combination where bedload and suspended load transport are occurring at different times or for different grain sizes. The Eaton and Church (2011) formula relies on a dimensionless critical specific stream power that is dependent on flow roughness – an impediment to network scale application. For the dataset used in this study, assuming a constant value of  $\omega_{c*}$  of 0.1 is just as accurate as their approach. Using this constant value of  $\omega_{c*}$  facilitates application of the Eaton and Church (2011) bedload equation at the network scale.

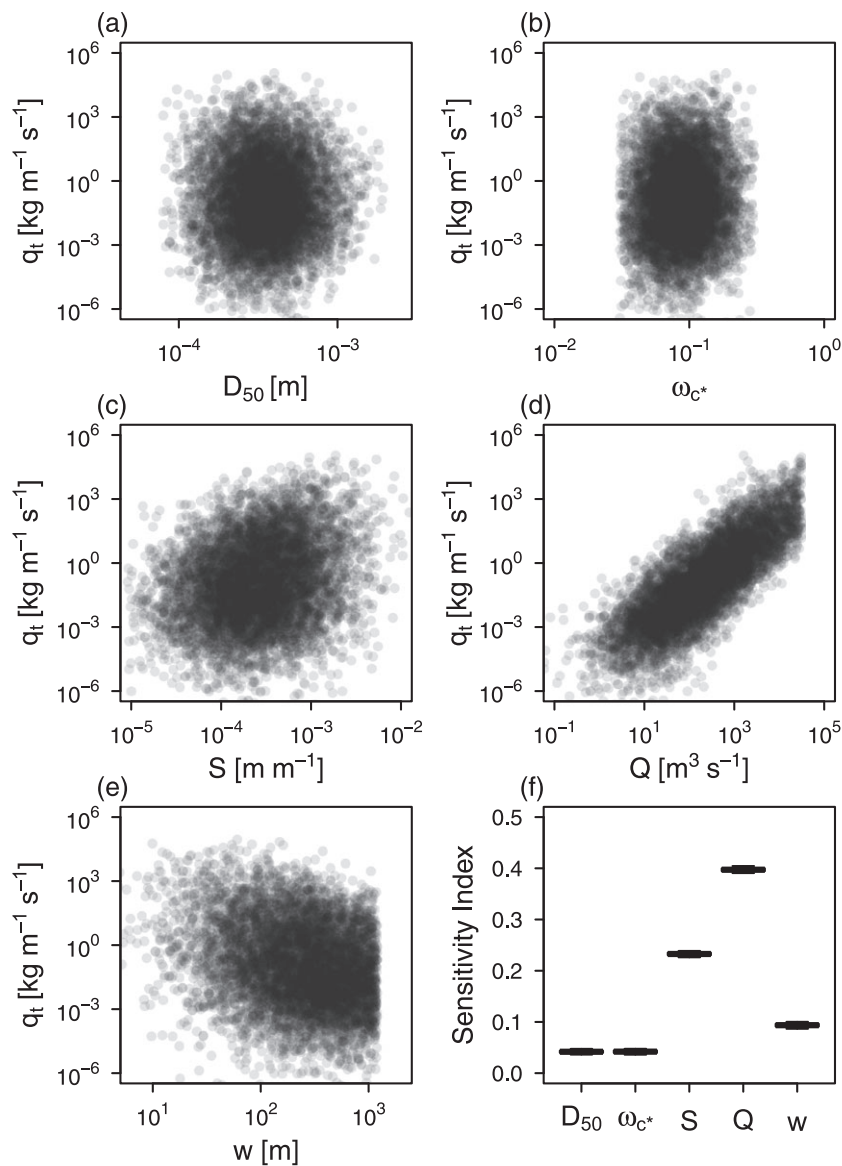


**Figure 7.** Scatterplots show simple correlation between simulated total transport rates and each of the five equation variables ( $N=7650$ ). Boxplot displays results of the formal sensitivity analysis of Equation (20) with bias-corrected values and uncertainty bounds based on bootstrapping with 1000 replicates.

### Uncertainty in sediment transport modeling

Much of the uncertainty in sediment transport modeling comes from uncertainty in the data used to parameterize transport formulae. The sensitivity results for both our new bedload and total load equations indicate that channel slope and discharge are the most important variables, while width, grain size, and  $\omega_{c^*}$  have only a small effect. This suggests that the accuracy of sediment flux predictions depends on a robust hydrologic foundation and accurate topographic data and is less dependent on accurately quantifying grain size – a variable that is rarely well defined throughout a channel network. Despite this, improvements in estimating variability in grain size at network scales would improve the applicability of these relations in addressing catchment management problems.

Sensitivity results are relatively consistent between the two equations, although grain size has a slightly higher influence in the bedload formula. This could be due to differences in equation structure as well as the much smaller range of grain sizes in the total load dataset. The relative unimportance of

grain size suggests that observed uncertainty in  $\omega_c$  (Figure 3) should have relatively little influence on calculated transport rates. Equation (15), however, was most accurate for finer grain sizes (sand and fine to medium gravel), suggesting that this equation may be better suited for fine grained streams. In addition, coarse grained streams are more likely to be near threshold conditions where uncertainty in  $\omega_c$  will produce greater uncertainty in transport rates.

Uncertainty in sediment transport rates translates directly to uncertainty in incision modeling. Quantifying this uncertainty is important but is less feasible with complicated models that require long run times. Also, models which require hydraulic modeling are subject to additional sources of uncertainty (e.g. flow resistance equations and cross-section geometry). Our simple stream power-based approach avoids these issues; however, morphodynamic models incorporating hydraulics are based on rigorous and physically-based principles and are likely to perform better in many situations if inputs, parameters, and boundary conditions can be specified with sufficient accuracy.

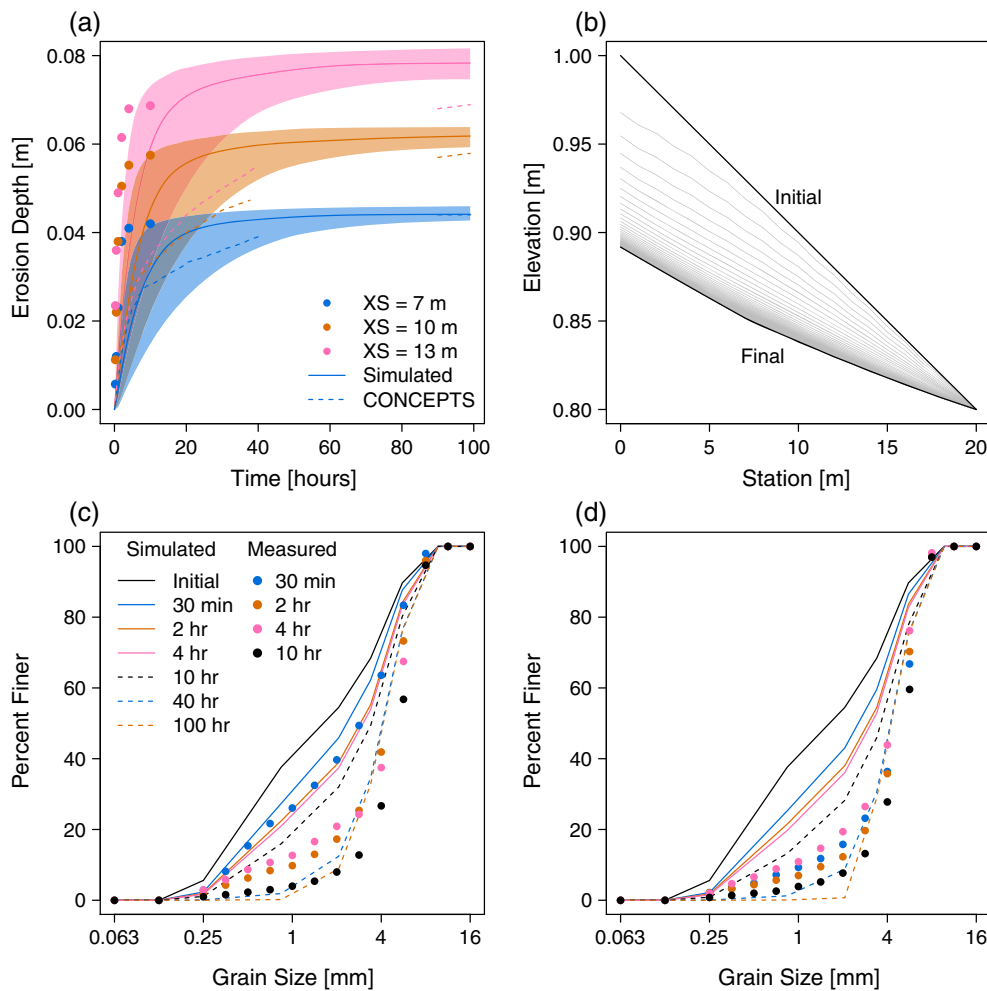


**Figure 8.** Results of incision modeling using the bedload equation (Equation (15)). (a) Observed erosion depths 7, 10, and 13 m from the downstream end compared with our simulations (with shaded uncertainty bounds) and those of CONCEPTS; (b) modeled evolution of the channel bed over time; and observed and simulated changes in grain size distributions over time 10 m (c) and 13 m (d) from the downstream end. [Colour figure can be viewed at [wileyonlinelibrary.com](http://wileyonlinelibrary.com)]

## Conclusions

We developed new bedload (Equation (15)) and total load (Equation (20)) sediment transport equations based on specific stream power and with no flow depth term. These equations can be used with only limited data: channel slope, discharge, width, and bed grain size. Using a comprehensive dataset from the literature on bedload and total load transport rates, we show that these new transport equations perform well compared with other formulae and represent a viable alternative to more complex equations requiring flow depth, flow resistance equations, or grain sorting. In addition, our results for flume data are consistent with previous studies indicating that dimensionless critical specific stream power for incipient motion is not strongly correlated with slope and has a mean value of  $\sim 0.1$  (Parker et al., 2011). Using this mean value allows critical specific stream power to be calculated using only grain size.

This work expands upon a rich history of relating sediment transport rates to stream power, beginning with Bagnold (1966). Others have built upon Bagnold's original approach, developing alternative bedload equations (Martin and Church, 2000; Parker, 2010; Eaton and Church, 2011) and exploring critical specific stream power as an alternative to critical shear stress (Parker et al., 2011; Camenen, 2012; Ferguson, 2012). We have contributed to this legacy, notably by developing a pair of bedload and total load equations that account for multiple modes of sediment transport. Still, much work remains to further test these equations and perhaps

develop dimensionally consistent versions following Martin and Church (2000). In addition, further investigation into the relationship between  $\omega_c^*$  and slope could be beneficial to better understand grain incipient motion within a specific stream power framework.

These new parsimonious equations can simplify sediment transport modeling at the stream network scale. A catchment scale approach to managing river sediment regimes is important (Wohl et al., 2015); however, adequate tools are only now being developed. Our new transport equations can be added to this river management toolbox, enabling explicit quantification of riverine sediment flux – a fundamental process affecting water quality, infrastructure operation, flood risk, habitat suitability, and channel morphodynamics.

**Acknowledgements**—This work was partially funded by the National Science Foundation, Integrative Graduate Education and Research Traineeship (IGERT) Grant No. DGE-0966346 'I-WATER: Integrated Water, Atmosphere, Ecosystems Education and Research Program' at Colorado State University. Additional funding was provided by the United States Environmental Protection Agency (USEPA) grant RD835570. Its contents are solely the responsibility of the grantee and do not necessarily represent the official views of the USEPA. Further, USEPA does not endorse the purchase of any commercial products or services mentioned in the publication. We are grateful to M. Church and C. Parker for sharing their compiled bedload transport databases. We also thank P. Nelson for assisting with the channel incision modeling. Finally, we appreciate the comments of two anonymous reviewers which greatly improved the quality of this paper.

## NOTATION

$A_s$	Area of the active layer
$C_{adj}, C_{orig}$	Adjusted and original coefficients from log-log linear regression fits
$D_{50, ref}$	Bagnold's reference median grain size (m)
$D_{50}$	Median grain size (m)
$D_c$	Adjusted critical grain size
$D_m$	Geometric mean grain size
$D_s$	Representative grain size (m)
$E^*$	Dimensionless transport parameter
$g$	Gravitational acceleration ( $\text{m s}^{-2}$ )
$h_{ref}$	Bagnold's reference flow depth (m)
$h$	Flow depth (m)
$n$	Sample size
$p$	Number of model parameters
$p_s$	Surface grain size proportion
$p_{sub}$	Subsurface grain size proportion
$Q$	Discharge ( $\text{m}^3 \text{s}^{-1}$ )
$q$	Unit discharge ( $\text{m}^2 \text{s}^{-1}$ )
$Q_t$	Total sediment load (ppm)
$q_{b, ref}$	Bagnold's reference unit bedload transport rate ( $\text{kg m}^{-1} \text{s}^{-1}$ )
$q_b$	Unit bedload transport rate ( $\text{kg m}^{-1} \text{s}^{-1}$ dry weight)
$q_b^*$	Dimensionless unit bedload transport rate
$q_t$	Unit total load transport rate ( $\text{kg m}^{-1} \text{s}^{-1}$ dry weight)
$\frac{\partial q}{\partial x}$	Change in sediment transport rate with distance
$S$	Water surface slope (m/m)
$s$	Sediment specific gravity (2.65)
$V$	Velocity ( $\text{m s}^{-1}$ )
$w$	Channel width (m)
$\frac{\partial z}{\partial t}$	Change in bed elevation with time
$\gamma$	Unit weight of water ( $\text{N m}^{-3}$ )
$\delta_s$	Active layer thickness
$\eta$	Hiding coefficient
$\theta_c$	Critical Shields parameter (dimensionless)
$\lambda$	Bed porosity
$\rho$	Fluid density ( $\text{kg m}^{-3}$ )
$\rho_r$	Submerged sediment density ( $\text{kg m}^{-3}$ )
$\rho_s$	Sediment density ( $\text{kg m}^{-3}$ )
$\tau$	Shear stress (Pa)
$\Omega$	Unit-length stream power ( $\text{W m}^{-1}$ )
$\omega$	Specific stream power ( $\text{kg m}^{-1} \text{s}^{-1}$ or $\text{W m}^{-2}$ )
$\omega^*$	Dimensionless specific stream power
$\omega_c$	Critical specific stream power ( $\text{kg m}^{-1} \text{s}^{-1}$ or $\text{W m}^{-2}$ )
$\omega_c^*$	Dimensionless critical specific stream power
$(\omega - \omega_c)_{ref}$	Bagnold's reference excess stream power ( $\text{kg m}^{-1} \text{s}^{-1}$ )

## References

- Ackers P, White WR. 1973. Sediment transport: New approach and analysis. *Journal of the Hydraulics Division* **99**: 2041–2060.
- Almedeij JH. 2002. Bedload transport in gravel-bed streams under a wide range of Shields stresses. PhD Dissertation, Virginia Polytechnic Institute.
- Ashida K, Michiue M. 1971. An investigation of river bed degradation downstream of a dam. *Proceedings of the 14th IAHR Congress*: Paris, 29 August–3 September.
- Bacchi V, Recking A, Eckert N, Frey P, Piton G, Naaim M. 2014. The effects of kinetic sorting on sediment mobility on steep slopes. *Earth Surface Processes and Landforms* **39**: 1075–1086. <https://doi.org/10.1002/esp.3564>.
- Bagnold RA. 1966. An approach to the sediment transport problem from general physics. USGS Professional Paper 422-I.
- Bagnold RA. 1973. The nature of saltation and of 'bed-load' transport in water. *Proceedings of the Royal Society of London A: Mathematical, Physical and Engineering Sciences* **332**: 473–504. <https://doi.org/10.1098/rspa.1983.0054>.
- Bagnold RA. 1977. Bed load transport by natural rivers. *Water Resources Research* **13**: 303–312. <https://doi.org/10.1029/WR013i002p00303>.
- Bagnold RA. 1980. An empirical correlation of bedload transport rates in flumes and natural rivers. *Proceedings of the Royal Society of London: Series A, Mathematical and Physical Sciences* **372**: 453–473.
- Bathurst JC. 1979. Hydraulics of mountain rivers. Report CER78-79JCB-RML-DBS55. Department of Civil Engineering, Colorado State University, Fort Collins, CO.
- Bathurst JC. 2013. Critical conditions for particle motion in coarse bed materials of nonuniform size distribution. *Geomorphology* **197**: 170–184. <https://doi.org/10.1016/j.geomorph.2013.05.008>.
- Bathurst JC, Graf WH, Cao HH. 1987. Bed load discharge equations for steep mountain rivers. In *Sediment Transport in Gravel-Bed Rivers*, Thorne CR, Bathurst JC, Hey RD (eds). John Wiley & Sons: Chichester; 453–492.
- Bizzi S, Lerner DN. 2015. The use of stream power as an indicator of channel sensitivity to erosion and deposition processes. *River Research and Applications* **31**: 16–27. <https://doi.org/10.1002/rra.2717>.
- Bravo-Espinosa M. 1999. Prediction of bedload discharge for alluvial channels. PhD. Dissertation, University of Arizona.
- Brownlie WR. 1981. *Compilation of alluvial channel data: laboratory and field*. WM Keck Laboratory of Hydraulics and Water Resources, California Institute of Technology.
- Brownlie WR. 1982. Prediction of flow depth and sediment discharge in open channels. PhD Dissertation, California Institute of Technology.
- Camenen B. 2012. Discussion of 'Understanding the influence of slope on the threshold of coarse grain motion: Revisiting critical stream power' by C Parker, NJ Clifford, and C.R. Thorne Geomorphology, Volume 126, March 2011, Pages 51–65. *Geomorphology* **139–140**: 34–38. <https://doi.org/10.1016/j.geomorph.2011.10.033>.
- Dey S, Raju UV. 2002. Incipient motion of gravel and coal beds. *Sadhana* **27**: 559–568. <https://doi.org/10.1007/BF02703294>.
- Eaton BC, Church M. 2011. A rational sediment transport scaling relation based on dimensionless stream power. *Earth Surface Processes and Landforms* **36**: 901–910. <https://doi.org/10.1002/esp.2120>.
- Engelund F, Hansen E. 1967. *A Monograph on Sediment Transport in Alluvial Streams*. Teknisk Forlag Technical Press: Copenhagen, Denmark.
- Ferguson R. 2007. Flow resistance equations for gravel- and boulder-bed streams. *Water Resources Research* **43**: W05427. <https://doi.org/10.1029/2006WR005422>.
- Ferguson RI. 1986. River loads underestimated by rating curves. *Water Resources Research* **22**: 74–76.
- Ferguson RI. 2005. Estimating critical stream power for bedload transport calculations in gravel-bed rivers. *Geomorphology* **70**: 33–41. <https://doi.org/10.1016/j.geomorph.2005.03.009>.
- Ferguson RI. 2012. River channel slope, flow resistance, and gravel entrainment thresholds. *Water Resources Research* **48**: W05517. <https://doi.org/10.1029/2011WR010850>.
- Frey P, Church M. 2011. Bedload: a granular phenomenon. *Earth Surface Processes and Landforms* **36**: 58–69. <https://doi.org/10.1002/esp.2103>.
- Garbrecht J, Kuhnle R, Alonso C. 1995. A sediment transport capacity formulation for application to large channel networks. *Journal of Soil and Water Conservation* **50**: 527–529.
- Gomez B, Church M. 1988. *A catalogue of equilibrium bedload transport data for coarse sand and gravel-bed channels*. University of British Columbia: Vancouver, B.C.
- Gomez B, Church M. 1989. An assessment of bed load sediment transport formulae for gravel bed rivers. *Water Resources Research* **25**: 1161–1186. <https://doi.org/10.1029/WR025i006p01161>.
- Habersack HM, Laronne JB. 2002. Evaluation and improvement of bed load discharge formulas based on Helleys-Smith sampling in an alpine gravel bed river. *Journal of Hydraulic Engineering* **128**: 484–499. [https://doi.org/10.1061/\(ASCE\)0733-9429\(2002\)128:5\(484\)](https://doi.org/10.1061/(ASCE)0733-9429(2002)128:5(484)).
- Hinton D, Hotchkiss R, Ames DP. 2016. Sediment transport database HydroServer [online] Available from: <http://worldwater.bryu.edu/app/index.php/sediment> (Accessed 20 May 2016)
- Hirsch C. 2007. *Numerical Computation of Internal and External Flows*, 2nd edn. Butterworth-Heinemann: Oxford.

- Ikeda H. 1983. Experiments on bedload transport, bed forms, and sedimentary structures using fine gravel in the 4-metre-wide flume. Paper 2. Environmental Research Center, University Tsukuba, Ibaraki, Japan.
- Ikeda S. 1982. Incipient motion of sand particles on side slopes. *Journal of the Hydraulics Division* **108**: 95–114.
- Johnson JW. 1943. Laboratory investigations on bedload transportation and bed roughness. Technical Paper 50, United States Agricultural Service, Soil Conservation Service.
- King JG, Emmett WW, Whiting PJ, Kenworthy RP, Barry JJ. 2004. Sediment transport data and related information for selected coarse-bed streams and rivers in Idaho. US Forest Service Report RMRS-GTR-131. [online] Available from: <http://www.fs.fed.us/rm/boise/research/watershed/BAT/>
- Lamb MP, Dietrich WE, Venditti JG. 2008. Is the critical Shields stress for incipient sediment motion dependent on channel-bed slope? *Journal of Geophysical Research: Earth Surface* **113** F02008. <https://doi.org/10.1029/2007JF000831>.
- Langendoen EJ, Alonso CV. 2008. Modeling the evolution of incised streams: I. Model formulation and validation of flow and streambed evolution components. *Journal of Hydraulic Engineering* **134**: 749–762. [https://doi.org/10.1016/ASCE\)0733-9429\(2008\)134:6\(749\)](https://doi.org/10.1016/ASCE)0733-9429(2008)134:6(749).
- Lea DM, Legleiter CJ. 2016. Mapping spatial patterns of stream power and channel change along a gravel-bed river in northern Yellowstone. *Geomorphology* **252**: 66–79. <https://doi.org/10.1016/j.geomorph.2015.05.033>.
- Martin Y. 2003. Evaluation of bed load transport formulae using field evidence from the Vedder River, British Columbia. *Geomorphology* **53**: 75–95. [https://doi.org/10.1016/S0169-555X\(02\)00348-3](https://doi.org/10.1016/S0169-555X(02)00348-3).
- Martin Y, Church M. 2000. Re-examination of Bagnold's empirical bedload formulae. *Earth Surface Processes and Landforms* **25**: 1011–1024. [https://doi.org/10.1002/1096-9837\(200008\)25:9<101::AID-ESP114>3.0.CO;2-H](https://doi.org/10.1002/1096-9837(200008)25:9<101::AID-ESP114>3.0.CO;2-H).
- Martin Y, Ham D. 2005. Testing bedload transport formulae using morphologic transport estimates and field data: lower Fraser River, British Columbia. *Earth Surface Processes and Landforms* **30**: 1265–1282. <https://doi.org/10.1002/esp.1200>.
- Meyer-Peter R, Müller R. 1948. Formulas for bedload transport. *Proceedings of the 2nd Meeting of the International Association of Hydraulic Research*: Stockholm, 39–64.
- Mizuyama T. 1977. Bedload transport in steep channels, PhD Dissertation, Kyoto University.
- Newson MD, Newson CL. 2000. Geomorphology, ecology and river channel habitat: Mesoscale approaches to basin-scale challenges. *Progress in Physical Geography* **24**: 195–217. <https://doi.org/10.1191/030913300760564724>.
- Owens PN. 2005. Conceptual models and budgets for sediment management at the river basin scale. *Journal of Soils and Sediments* **5**: 201–212. <https://doi.org/10.1065/jss2005.05.133>.
- Parker C. 2010. Quantifying catchment-scale coarse sediment dynamics in British rivers, PhD Dissertation, University of Nottingham.
- Parker C, Clifford NJ, Thorne CR. 2011. Understanding the influence of slope on the threshold of coarse grain motion: revisiting critical stream power. *Geomorphology* **126**: 51–65. <https://doi.org/10.1016/j.geomorph.2010.10.027>.
- Parker C, Clifford NJ, Thorne CR. 2012. Automatic delineation of functional river reach boundaries for river research and applications. *River Research and Applications* **28**: 1708–1725. <https://doi.org/10.1002/rra>.
- Parker C, Thorne CR, Clifford NJ. 2015. Development of ST:REAM: a reach-based stream power balance approach for predicting alluvial river channel adjustment. *Earth Surface Processes and Landforms* **40**: 403–413. <https://doi.org/10.1002/esp.3641>.
- Parker G. 1990. Surface-based bedload transport relation for gravel rivers. *Journal of Hydraulic Research* **28**: 417–436. <https://doi.org/10.1080/00221689009499058>.
- Parker G, Klingeman PC, McLean DG. 1982. Bedload and size distribution in paved gravel-bed streams. *Journal of the Hydraulics Division ASCE* **108**: 544–571.
- Phillips RTJ, Desloges JR. 2014. Glacially conditioned specific stream powers in low-relief river catchments of the southern Laurentian Great Lakes. *Geomorphology* **206**: 271–287. <https://doi.org/10.1016/j.geomorph.2013.09.030>.
- Plischke E, Borgonovo E, Smith CL. 2013. Global sensitivity measures from given data. *European Journal of Operational Research* **226**: 536–550. <https://doi.org/10.1016/j.ejor.2012.11.047>.
- Prancevic JP, Lamb MP. 2015. Unraveling bed slope from relative roughness in initial sediment motion. *Journal of Geophysical Research: Earth Surface* **120**: 474–489. <https://doi.org/10.1002/2014JF003323>.
- Prancevic JP, Lamb MP, Fuller BM. 2014. Incipient sediment motion across the river to debris-flow transition. *Geology* **42**: 191–194.
- R Core Team. 2016. R: a language and environment for statistical computing. R Foundation for Statistical Computing: Vienna, Austria.
- Recking A. 2009. Theoretical development on the effects of changing flow hydraulics on incipient bed load motion. *Water Resources Research* **45** W04401. <https://doi.org/10.1029/2008WR00826>.
- Recking A. 2013. Simple method for calculating reach-averaged bed-load transport. *Journal of Hydraulic Engineering* **139**: 70–75. [https://doi.org/10.1016/ASCE\)HY.1943-7900.0000653](https://doi.org/10.1016/ASCE)HY.1943-7900.0000653).
- Reinfelds I, Cohen T, Batten P, Brierley G. 2003. Assessment of downstream trends in channel gradient, total and specific stream power: a GIS approach. *Geomorphology* **60**: 403–416. <https://doi.org/10.1016/j.geomorph.2003.10.003>.
- Rice SP, Greenwood MT, Joyce CB. 2001. Tributaries, sediment sources, and the longitudinal organisation of macroinvertebrate fauna along river systems. *Canadian Journal of Fisheries and Aquatic Sciences* **58**: 824–840. <https://doi.org/10.1139/f01-022>.
- Saad MBEA. 1989. Critical shear stress of armour coat. In *Sediment Transport Modeling, Proceedings of the International Symposium*, Wang SSY (ed). American Society of Civil Engineers: New York; 308–313.
- Shields A. 1936. Awendung der Aehnlichkeitsmechanik und der Turbulenzforschung auf die Geschiebebewegung. *Preussischen Versuchsanstalt für Wasserbau* **26**: 26.
- Shvidchenko AB, Pender G. 2000. Initial motion of streambeds composed of coarse uniform sediments. *Proceedings of the Institution of Civil Engineers - Water Maritime and Energy* **142**: 217–227. <https://doi.org/10.1680/wame.2000.142.4.217>.
- Smith EP, Rose KA. 1995. Model goodness-of-fit analysis using regression and related techniques. *Ecological Modelling* **77**: 49–64. [https://doi.org/10.1016/0304-3800\(93\)E0074-D](https://doi.org/10.1016/0304-3800(93)E0074-D).
- Soulsby RL. 1997. *Dynamics of Marine Sands, a Manual for Practical Applications*. Thomas Telford: London, UK.
- Stover SC, Montgomery DR. 2001. Channel change and flooding, Skokomish River, Washington. *Journal of Hydrology* **243**: 272–286. [https://doi.org/10.1016/S0022-1694\(00\)00421-2](https://doi.org/10.1016/S0022-1694(00)00421-2).
- Taylor BD. 1971. Temperature effects in alluvial streams. Report KH-R-27, W.M. Keck Laboratory of Hydraulic and Water Resources, California, Institution Technic.
- Theil H. 1958. *Economic Forecasts and Policy*. North Holland: Amsterdam, Netherlands.
- Vanoni VA. 1975. *Sedimentation Engineering*. ASCE Manuals and Reports on Engineering Practice No. 54.
- Vázquez-Tarrio D, Menéndez-Duarte R. 2015. Assessment of bedload equations using data obtained with tracers in two coarse-bed mountain streams (Narcea River basin, NW Spain). *Geomorphology* **238**: 78–93. <https://doi.org/10.1016/j.geomorph.2015.02.032>.
- Wilcock PR, Crowe JC. 2003. Surface-based transport model for mixed-size sediment. *Journal of Hydraulic Engineering* **129**: 120–128.
- Williams GP. 1970. Flume width and water depth effects in sediment transport experiments. US Geological Survey Professional Paper 562-H
- Williams GP, Rosgen DL. 1989. Measured total sediment loads (suspended loads and bedloads) for 93 United States streams. US Geological Survey, Open-File Report 89–67.
- Wohl E, Bledsoe BP, Jacobson RB, Poff NL, Rathburn SL, Walters DM, Wilcox AC. 2015. The natural sediment regime in rivers: broadening the foundation for ecosystem management. *BioScience* **65**: 358–371. <https://doi.org/10.1093/biosci/biv002>.
- Yang CT. 1979. Unit stream power equations for total load. *Journal of Hydrology* **40**: 123–138. [https://doi.org/10.1016/0022-1694\(79\)90092-1](https://doi.org/10.1016/0022-1694(79)90092-1).
- Yang S, Hu J, Wang X. 2006. Incipient motion of coarse particles in high gradient rivers. *International Journal of Sediment Research* **21**: 220–229.

## Appendix

### Eaton and Church (2011) Critical stream power model

Eaton and Church (2011) developed a relatively simple equation for dimensionless critical specific stream power using Shield's parameter and a flow resistance parameter:

$$\omega_{c*} = \theta_c^{3/2} \Re \quad (\text{A1})$$

where  $\Re$  is the flow resistance value given as the ratio of flow velocity ( $V$ ) to shear velocity ( $u_* = \sqrt{\tau/\rho}$ ). Eaton and Church (2011) chose to approximate this value using a power law developed by Ferguson (2007):

$$\Re = \frac{V}{u_*} = a \left[ \frac{h}{D_s} \right]^b \quad (\text{A2})$$

where  $a$  and  $b$  are empirical parameters that vary with relative submergence (defined as  $h/D_{84}$ ). For 'deep' flows,  $a = 7-8$  and  $b = 1/6$  but for 'shallow' flows  $a = 1-4$  and  $b = 1$  (Ferguson, 2007). For our incipient motion analysis, we used measured values of  $V$  and  $u_*$  to calculate flow resistance which avoided the need to approximate this value using Ferguson's power relationship.

### Camenen (2012) Critical stream power model

Camenen (2012) defined a theoretical model for computing critical specific stream power:

$$\omega_c = \frac{2.3\rho}{\kappa} \left[ \left( \frac{R_h}{D_s} \right)_c \frac{\theta_{c,S}}{\theta_{c,0}} S g D_s \right]^{3/2} \log \left[ \frac{15}{e^1} \left( \frac{R_h}{D_s} \right)_c \right] \quad (\text{A3})$$

where  $\kappa = 0.4$  is the Von Karman constant and  $R_h$  is hydraulic radius. The critical relative flow depth (that is the flow depth at incipient motion) varies non-linearly with channel slope:

$$\left( \frac{R_h}{D_s} \right)_c = \frac{(s-1)\theta_{c,0}}{S} (0.5 + 6S^{0.75}) \quad (\text{A4})$$

where the subscript 0 in the critical Shields parameter indicates no slope effects. This value is a function of dimensionless grain size ( Soulsby, 1997):

$$\theta_{c,0} = \frac{0.30}{1 + 1.2D_*} + 0.055[1 - \exp(-0.02D_*)] \quad (\text{A5})$$

$$D_* = \left[ \frac{(s-1)g}{v^2} \right]^{1/3} D_s \quad (\text{A6})$$

Finally, the effect of slope on decreasing the critical Shields parameter as it approaches the angle of repose can be accounted for (Ikeda, 1982):

$$\frac{\theta_{c,S}}{\theta_{c,0}} = \frac{\sin(\phi_s - \arctan S)}{\sin(\phi_s)} = \cos(\arctan S) \left[ 1 - \frac{S}{\tan(\phi_s)} \right] \quad (\text{A7})$$

In this analysis, the angle of repose ( $\phi_s$ ) was assumed to equal 52° (Ferguson, 2012).

### Ferguson (2012) Critical stream power model

Ferguson's (2012) critical stream power model is based on the concept of hiding and protrusion in a streambed with non-

uniform grain size. Given this configuration, only a portion of the total shear stress is available to entrain small grains due to the additional grain roughness. The ratio of critical shear stress to the critical stress at a 'base resistance conditions' (i.e. no hiding and protrusion) is thus related to the ratio of critical flow depths:

$$\frac{\theta_c}{\theta_c'} = \frac{h_c}{h_c'} \quad (\text{A8})$$

where  $\theta_c'$  and  $h_c'$  are the critical Shields parameter and flow depth at the 'base resistance condition'. This relationship can also be expressed as a function of grain sorting and relative roughness:

$$\begin{aligned} \frac{\theta_c}{\theta_c'} &= \frac{h_c}{h_c'} \\ &= \left( \frac{a_o}{a_1} \right)^{3/2} \left( \frac{D_{84}}{D_{50}} \right)^{1/4} \left[ 1 + \left( \frac{a_1}{a_2} \right)^2 \left( \frac{D_{84}}{h} \right)^{5/3} \right]^{3/4} \end{aligned} \quad (\text{A9})$$

where  $a_o$ ,  $a_1$  and  $a_2$  are constants (assumed to be 8, 6.5 and 2.5, respectively). Slopes can then be found using the definition of the Shields parameter:

$$S = \frac{(s-1)\theta_c D_{50}}{h_c} = \frac{(s-1)(\theta_c/\theta_c')\theta_c'}{(h_c/D_{84})(D_{84}/D_{50})} \quad (\text{A10})$$

The effect of slope on the critical Shields parameter can be corrected, using the same approach as the Camenen model (Equation (A7)). In this case, the critical Shields parameter for a given slope must be solved iteratively using trial values of  $h_c/D_{84}$ . Once this critical value has been computed, the critical dimensionless stream power can be calculated using a similar approach to Eaton and Church (2011):

$$\omega_{c*} = \theta_c^{3/2} \frac{V}{u_*} \quad (\text{A11})$$

where  $V/u_*$  is computed using the variable-power flow resistance equation:

$$\frac{V}{u_*} = \frac{a_1(h/D_{84})}{\left[ (h/D_{84})^{5/3} + (a_1/a_2)^2 \right]^{1/2}} \quad (\text{A12})$$

where  $V$  is flow velocity ( $\text{m s}^{-1}$ ),  $u_*$  is shear velocity ( $\text{m s}^{-1}$ ), and  $a_1$  and  $a_2$  are constants (defined above).

### Ackers and White (1973) Total load equation

The Ackers and White total load equation takes the following form:

$$C_w = c \frac{\rho_s D_{50}}{\rho R_h} \left( \frac{V}{u_*} \right)^n \left[ F_{gr} - 1 \right]^m \quad (\text{A13})$$

where  $C_w$  is the sediment concentration by weight, and  $F_{gr}$  is the mobility number defined as:

$$F_{gr} = \frac{u_*^n u_*'^{1-n}}{\sqrt{g D_{50} \left( \frac{\rho_s - \rho}{\rho} \right)}} \quad (\text{A14})$$

and  $u_*'$  is:

$$u_*' = \frac{V}{\sqrt{32} \log \left( \frac{10R_h}{D_{50}} \right)} \quad (\text{A15})$$

the values of  $n$ ,  $A$ ,  $m$ , and  $c$  are functions of  $D_{gr}$  which is defined as:

$$D_{gr} = \left[ \sqrt{\frac{\rho_s - \rho}{\rho}} R_g \right]^{2/3} \quad (\text{A16})$$

where  $R_g$  is the Reynolds grain number:

$$R_g = \frac{\sqrt{g D_{50}^3}}{v} \quad (\text{A17})$$

when  $D_{gr} > 60$ , the coefficients are:

$$\begin{aligned} n &= 0.0 \\ A &= 0.17 \\ m &= 1.5 \\ c &= 0.025 \end{aligned} \quad (\text{A18})$$

If  $60 \geq D_{gr} \geq 1$  then:

$$\begin{aligned} n &= 1 - 0.56 \log D_{gr} \\ A &= \frac{0.23}{\sqrt{D_{gr}}} + 0.14 \\ m &= \frac{9.66}{D_{gr}} + 1.34 \\ \log c &= 2.86 \log D_{gr} - (\log D_{gr})^2 - 3.53 \end{aligned} \quad (\text{A19})$$

Engelund and Hansen (1967) Total load equation

The Engelund and Hansen (1967) total load equation is:

$$C_w = 0.05 \left( \frac{\rho_s}{\rho_s - \rho} \right) \left( \frac{VS}{\sqrt{\left( \frac{\rho_s - \rho}{\rho} \right) g D_{50}}} \right) \theta^{1/2} \quad (\text{A20})$$

where  $C_w$  is sediment concentration by weight and  $\theta$  is the Shields parameter.

Brownlie (1982) Total load equation

Brownlie's (1982) total load equation is:

$$C_{ppm} = 7115 C_f \left( \frac{V - V_c}{\sqrt{(s-1)g D_{50}}} \right)^{1.978} S^{0.6601} \left( \frac{R_h}{D_{50}} \right)^{-0.3301} \quad (\text{A21})$$

where  $C_{ppm}$  is the sediment concentration in ppm,  $C_f$  is a correction factor (1.0 for flume data and 1.268 for field data) and:

$$\frac{V_c}{\sqrt{(s-1)g D_{50}}} = 4.596 \theta_c^{0.529} S^{-0.1405} \sigma_g^{-0.1606}, \quad (\text{A22})$$

$$\sigma_g = \sqrt{\frac{D_{84}}{D_{16}}} \quad (\text{A23})$$

Brownlie fit a continuous function to the Shields curve to provide consistent estimates of  $\theta_c$ :

$$\begin{aligned} \theta_c &= 0.22 Y + 0.06 * 10^{-7.7Y}, \\ Y &= \left( \frac{\sqrt{(s-1)g D_{50}^3}}{v} \right)^{-0.6} \end{aligned} \quad (\text{A23})$$

Since hydraulic radius and grain size were given in the data used, we did not use Brownlie's depth predictor equations for this analysis.

## APPENDIX NOTATION

$a_o, a_1$ and $a_2$	Constants
$C_w$	Sediment concentration by weight
$D_{84}$	Grain size with 84% of the distribution finer (m)
$D_{16}$	Grain size with 16% of the distribution finer (m)
$D^*$	Dimensionless grain size
$F_{gr}$	Mobility number
$h_c$	Critical flow depth
$n, A, m$ , and $c$	Constants
$R_g$	Reynolds grain number
$R_h$	Hydraulic radius (m)
$u^*$	Shear velocity ( $m s^{-1}$ )
$V_c$	Critical velocity
$\theta_{c,s}$	Critical Shields parameter with slope effects
$\theta_{c,0}$	Critical Shields parameter with no slope effects
$\kappa$	Von Karman constant
$v$	Kinematic water viscosity ( $m^2 s^{-1}$ )
$\sigma_g$	Geometric standard deviation of grain sizes
$\phi_s$	Sediment angle of repose ( $^\circ$ )

## Supporting Information

Additional Supporting Information may be found online in the supporting information tab for this article.

**Table S1** contains all incipient motion data used in this analysis. **Table S2** contains all bedload data used with bedload transport rates adjusted as described in the text.

**Table S3** contains the filtered Brownlie (1981) total load dataset.